Electronic Supporting Information

Electron-Accepting π-Conjugated Systems for Organic Photovoltaics: Influence of Structural Modification on Molecular Orientation at Donor-Acceptor Interfaces

Seihou Jinnai, Yutaka Ie, Makoto Karakawa, Tom Aernouts, Yukihiro Nakajima, Shogo Mori, and Yoshio Aso

The Institute of Scientific and Industrial Research (ISIR), Osaka University, 8-1 Mihogaoka, Ibaraki, Osaka 567-0047, Japan
IMEC, Organic Photovoltaics, Kapeldreef 75, Leuven, Belgium
Division of Chemistry and Materials, Faculty of Textile Science and Technology, Shinshu University, 3-15-1 Tokida, Ueda, Nagano 386-8567, Japan

Table of Contents

Scheme and Figures

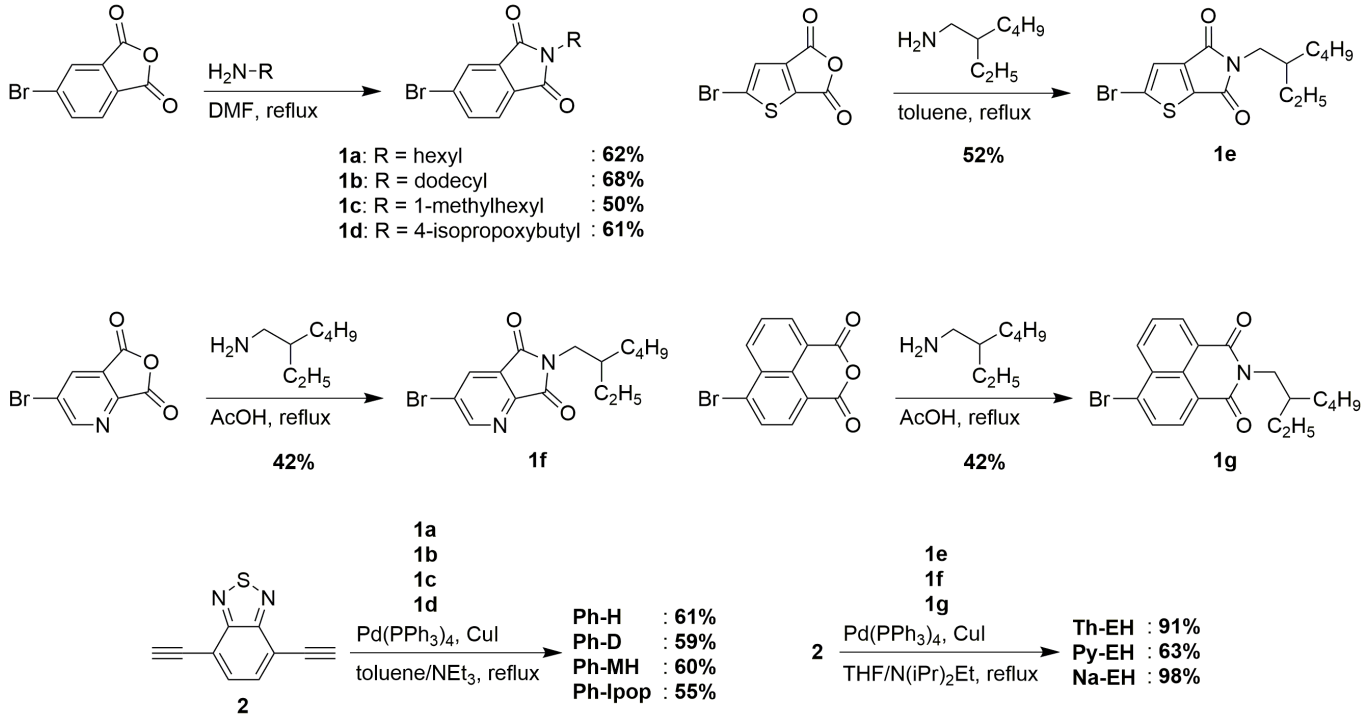

Scheme S1. Synthesis of target compounds.

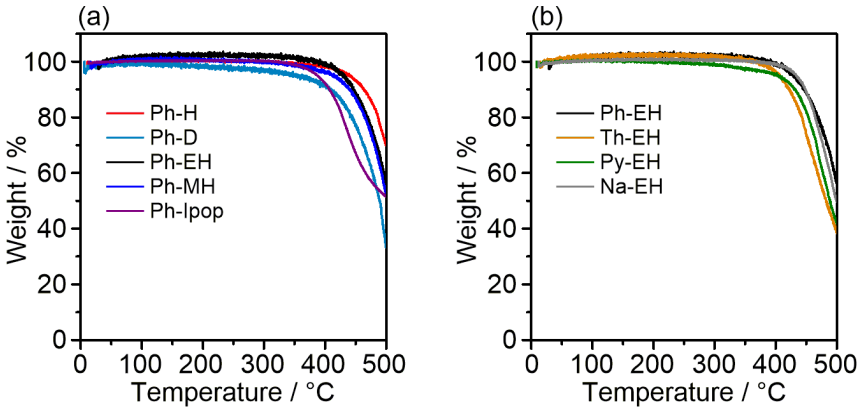

Figure S1. TGA curves of (a) Ph-X (X = H, D, EH, MH, and Ipop) and (b) Ar-EH (Ar = Ph, Th, Py, and Na) with a scanning rate of 10 °C min^{-1} under N_2.

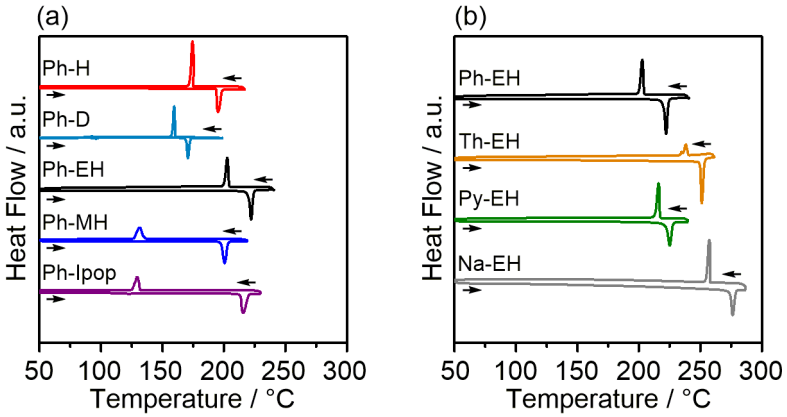

Figure S2. DSC thermograms of (a) Ph-X (X = H, D, EH, MH, and Ipop) and (b) Ar-EH (Ar = Ph, Th, Py, and Na) with a scanning rate of 10 °C min^{-1} under N_2.

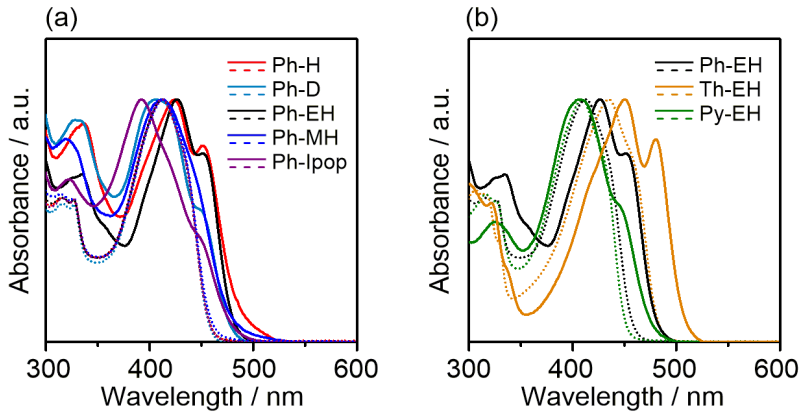

Figure S3. UV-Vis absorption spectra of (a) Ph-X (X = H, D, EH, MH, and Ipop) and (b) Ar-EH (Ar = Ph, Th, and Py) in a $CHCl_3$ solution (dashed line) and in a film state (solid line).

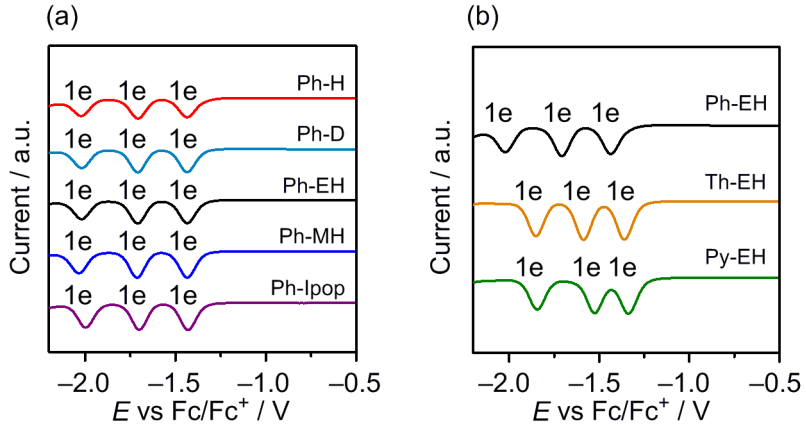

Figure S4. Differential pulse voltammograms of (a) Ph-X (X = H, D, EH, MH, and Ipop) and (b) Ar-EH (Ar = Ph, Th, and Py), measured in *o*-DCB/acetonitrile (5/1) containing 0.1 M $TBAPF_6$.

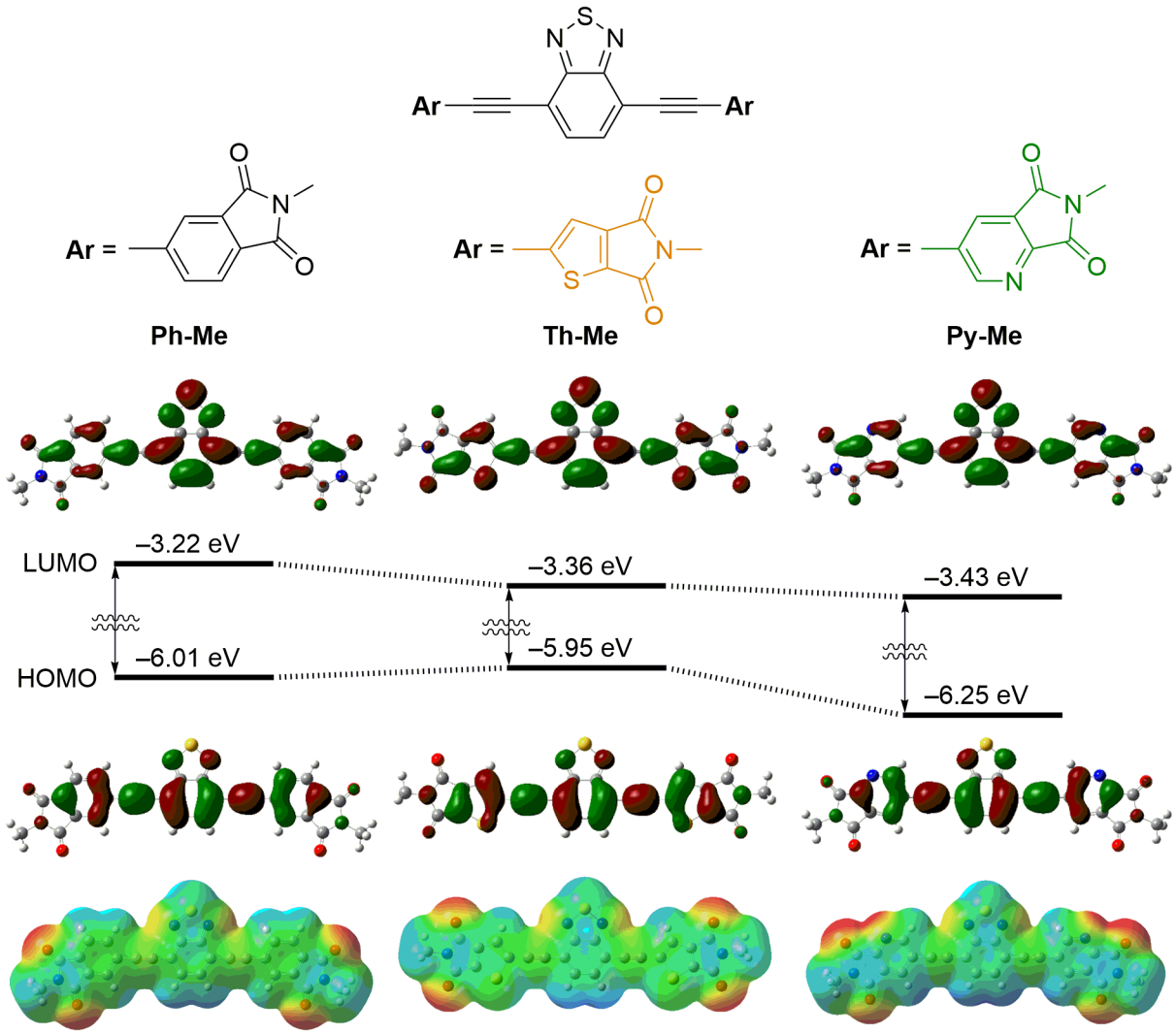

Figure S5. HOMO, LUMO, and ESP of model compounds calculated using DFT at the B3LYP/6-31G (d, p) level.

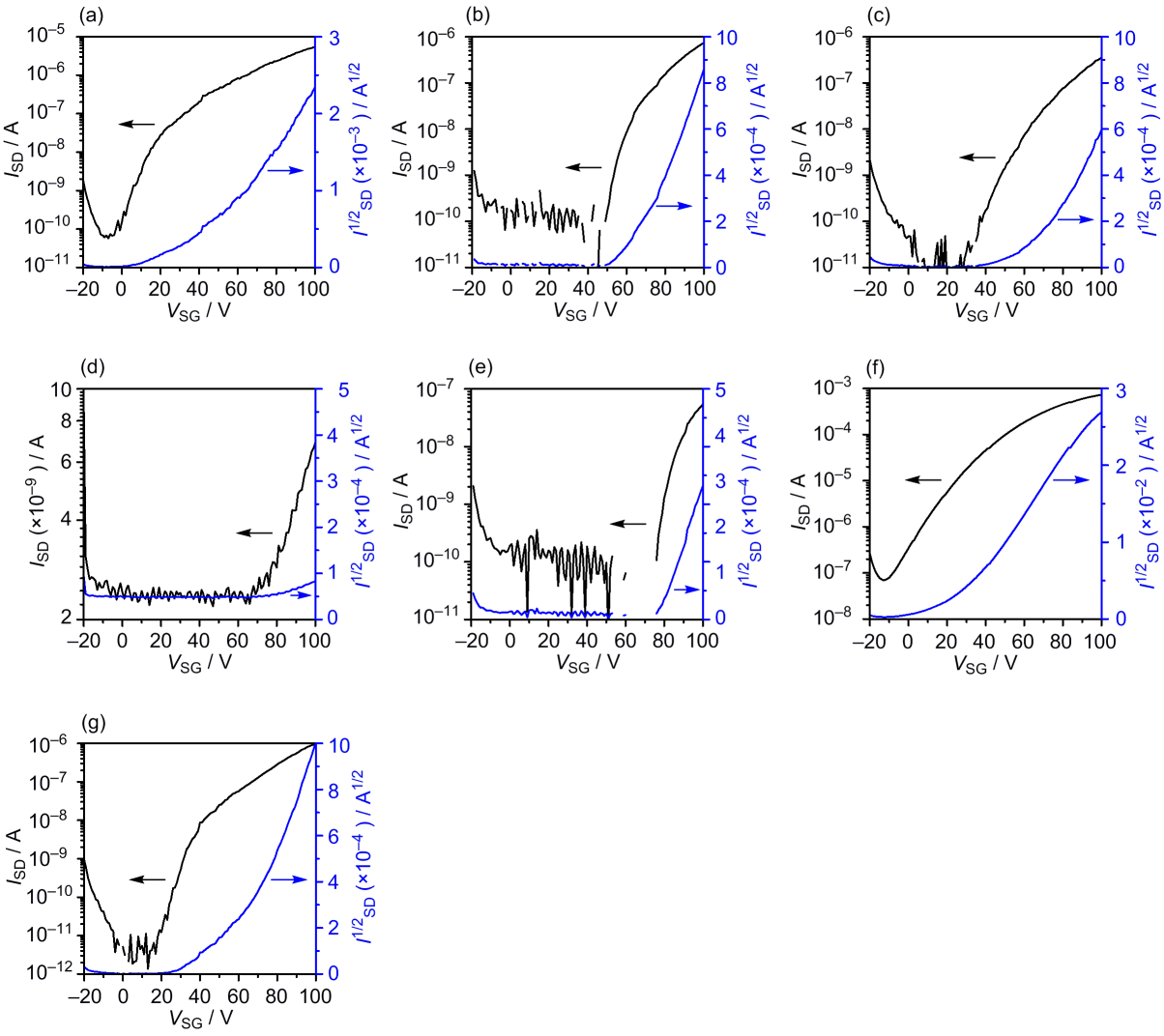

Figure S6. Transfer characteristics of (a) Ph-H, (b) Ph-D, (c) Ph-EH, (d) Ph-MH, (e) Ph-Ipop, (f) Th-EH, and (g) Py-EH -based OFETs. I_{SD} and V_{SG} denote source-drain current and gate voltage, respectively.

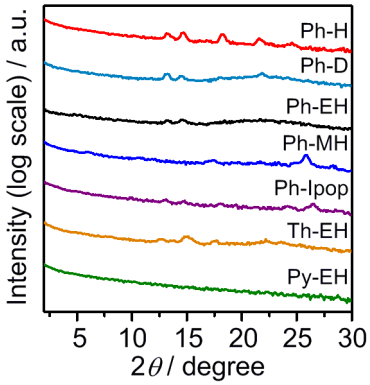

Figure S7. In-plane X-ray diffractograms of Ph-X (X = H, D, EH, MH, and Ipop) and Ar-EH (Ar = Th and Py) films.

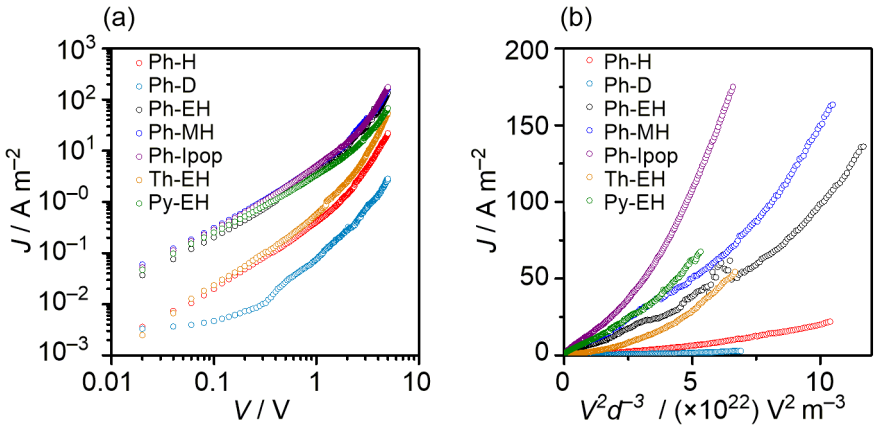

Figure S8. (a) *J*–*V* and (b) *J*–V^2d^{-3} characteristics of electron-only devices for Ph-X (X = H, D, EH, MH, and Ipop) and Ar-EH (Ar = Th and Py) films.

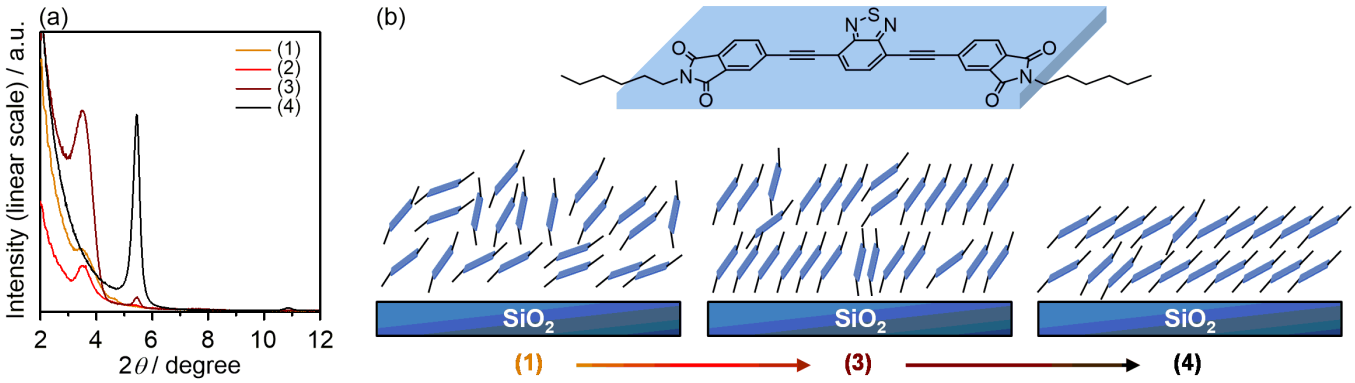

Figure S9. (a) Out-of-plane X-ray diffractograms of Ph-H-based films coated on (1) bare SiO_2, (2) HMDS-modified SiO_2, (3) ODTS-modified SiO_2, and (4) thermally annealed film of (3). (b) Graphical representation of the molecular orientation in conditions (1), (3), and (4).

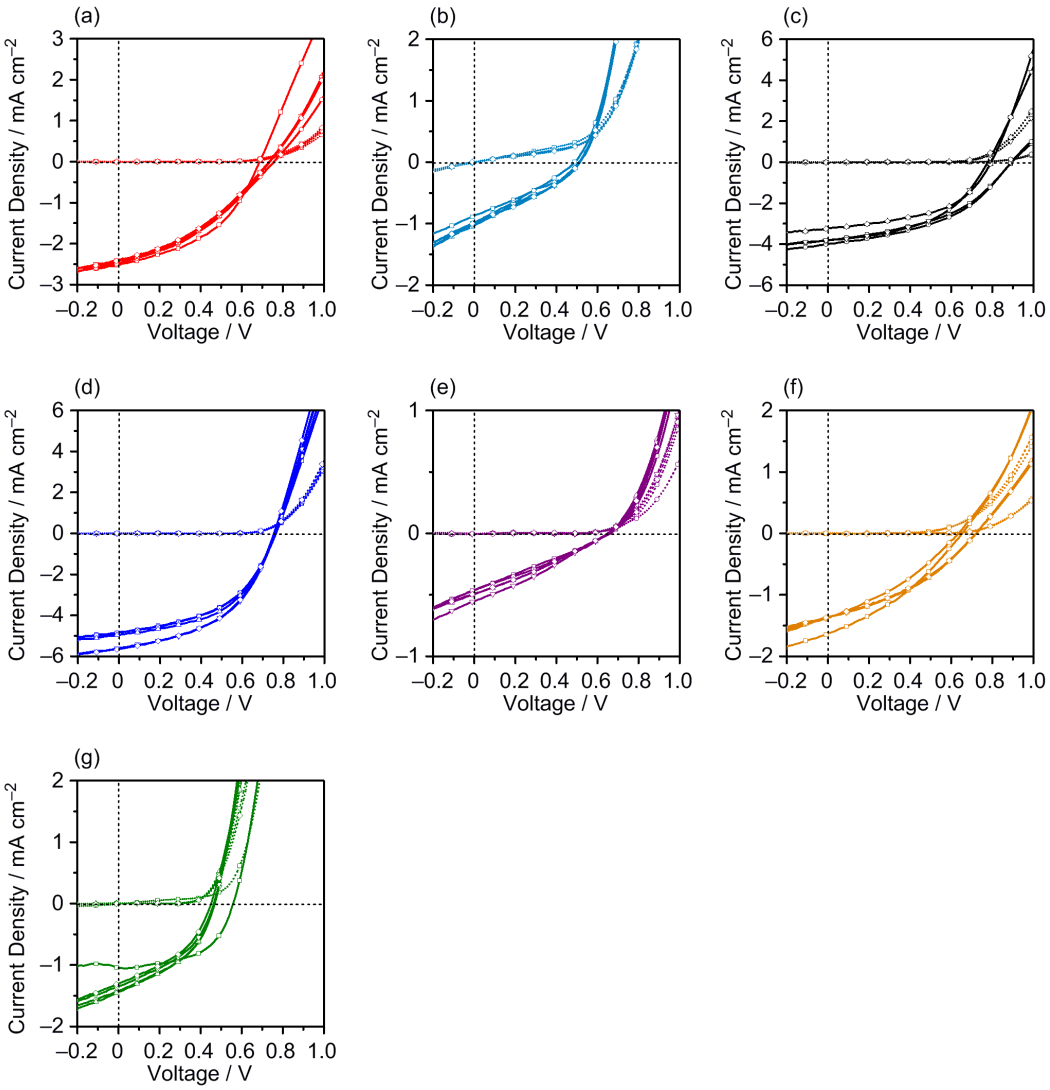

Figure S10. *J–V* curves of OPV devices for (a) P3HT/Ph-H, (b) P3HT/Ph-D, (c) P3HT/Ph-EH, (d) P3HT/Ph-MH, (e) P3HT/Ph-Ipop, (f) P3HT/Th-EH, and (g) P3HT/Py-EH films.

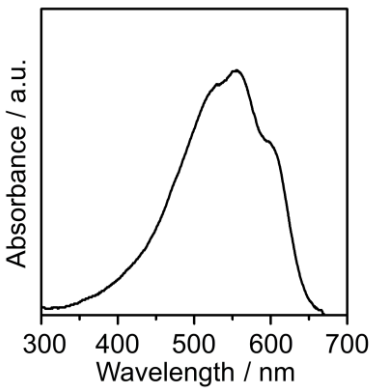

Figure S11. UV-Vis absorption spectrum of P3HT film.

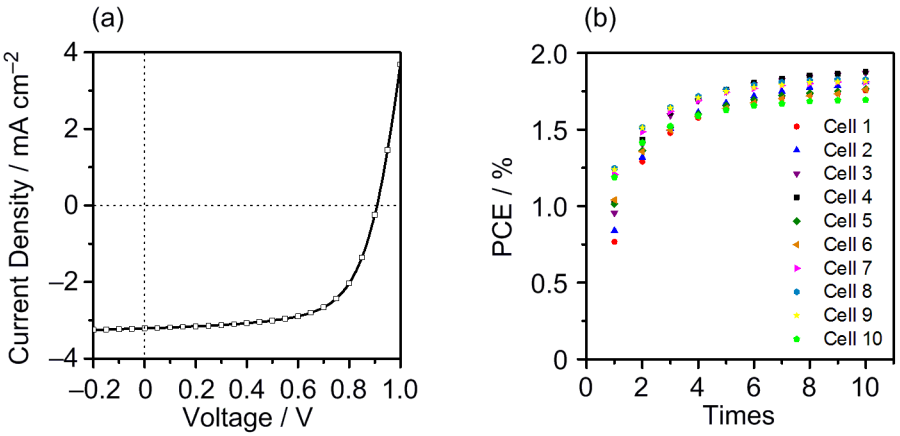

Figure S12. (a) *J–V* curve inverted type OPV device with a structure of ITO/TiO_x/P3HT:Ph-MH/MoO_x/Ag and (b) repeated *J–V* characteristics of ten devices.[1]

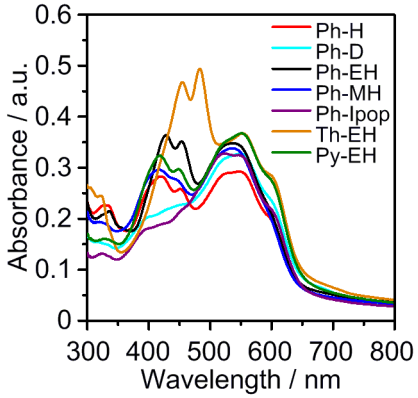

Figure S13. UV-Vis absorption spectra of the P3HT/acceptor blend films.

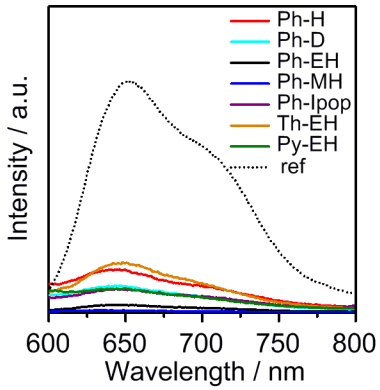

Figure S14. Fluorescence spectra of the P3HT/acceptor blend films.

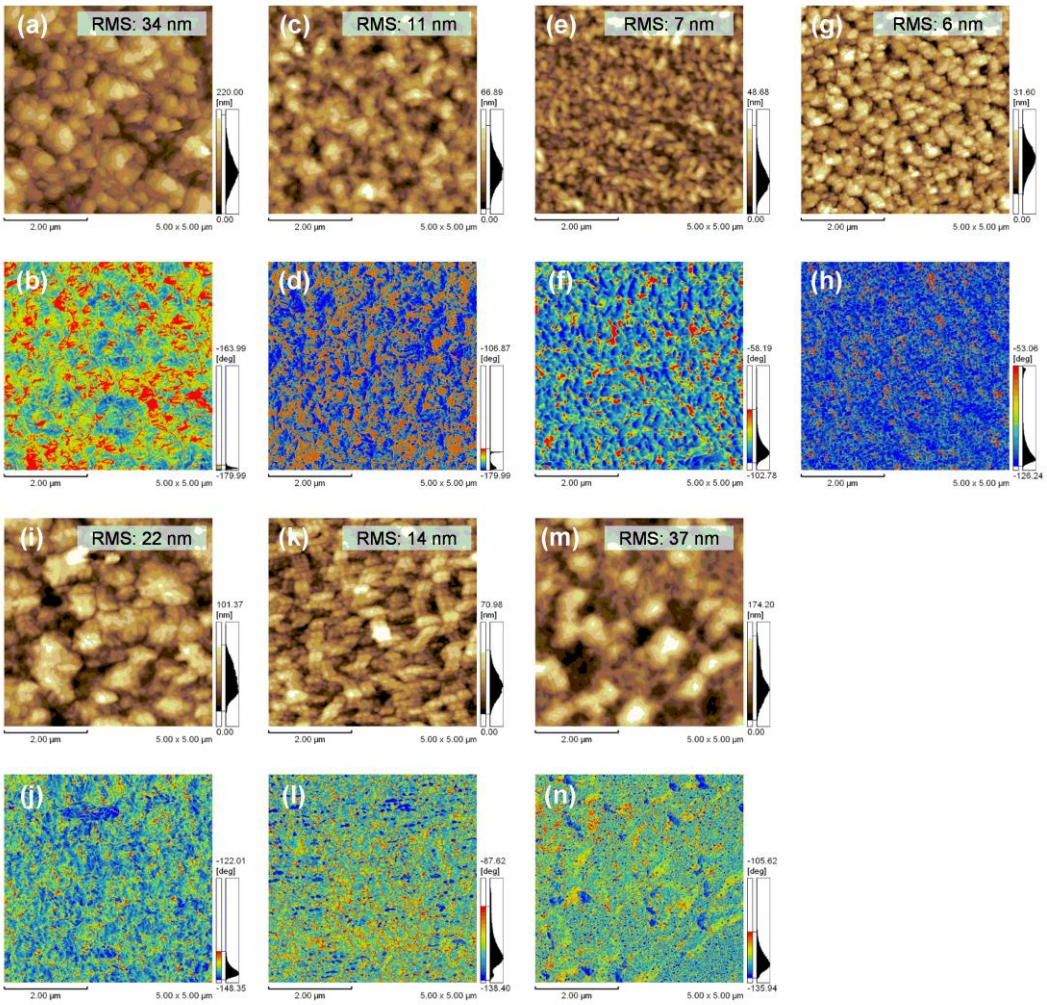

Figure S15. AFM height and phase images of (a, b) P3HT/Ph-H, (c, d) P3HT/Ph-D, (e, f) P3HT/Ph-EH, (g, h) P3HT/Ph-MH, (i, j) P3HT/Ph-Ipop, (k, l) P3HT/Th-EH, and (m, n) P3HT/Py-EH blend films.

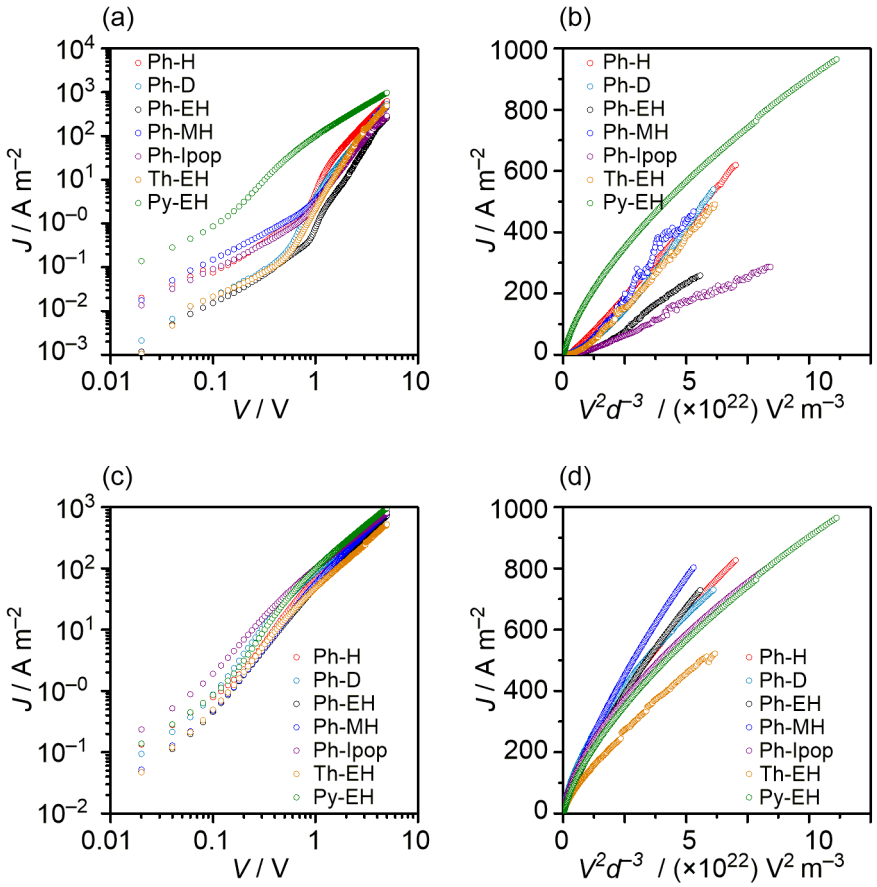

Figure S16. (a) *J*–*V* and (b) *J*–V^2d^{-3} characteristics of electron-only devices and (c) *J*–*V* and (d) *J*–V^2d^{-3} characteristics of hole-only devices for Ph-X (X = H, D, EH, MH, and Ipop) and Ar-EH (Ar = Th and Py) films.

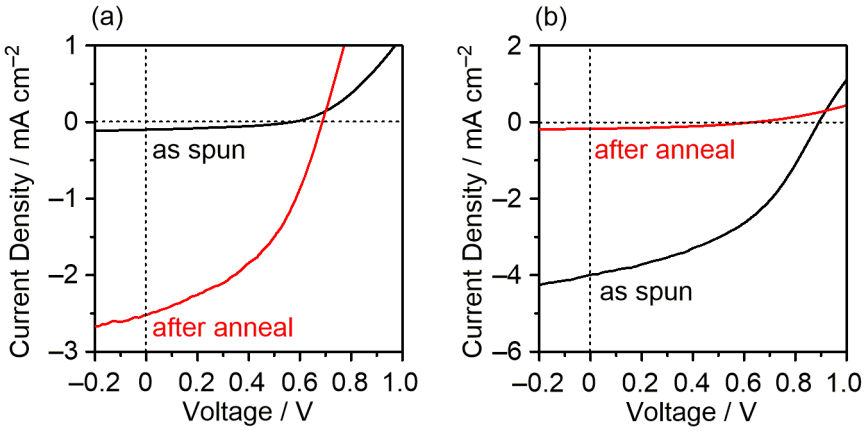

Figure S17. *J*–*V* characteristics of OPV devices for (a) P3HT/Ph-H and (b) P3HT/Ph-EH films before and after thermal annealing.

Table S1. Field-effect characteristics and SCLC electron mobilities of Ph-X- and Ar-EH-based films.

	T_a /°C	$\mu_{e,\ FET}$ /cm^2 V^{-1} s^{-1}	I_{on}/I_{off}	V_{th} /V	$\mu_{e,\ SCLC}$ /cm^2 V^{-1} s^{-1}
Ph-H	160	3.4×10^{-5}	10^5	67	8.0×10^{-8}
Ph-D	190	9.3×10^{-6}	10^3	63	1.1×10^{-8}
Ph-EH	160	5.4×10^{-6}	10^3	70	3.3×10^{-7}
Ph-MH	130	4.1×10^{-8}	3	47	5.0×10^{-7}
Ph-Ipop	190	1.9×10^{-6}	10^2	78	1.1×10^{-6}
Th-EH	160	4.9×10^{-4}	10^4	38	3.7×10^{-7}
Py-EH	160	1.1×10^{-5}	10^5	62	4.7×10^{-7}

Table S2. OFET characteristics and SFE data of Ph-H films.

condition	treatment	T_a/°C	μ_e/cm^2 V^{-1} s^{-1}	θ_{water} /°	$\theta_{glycerol}$ /°	γ^d /mJ cm^{-2}	γ^p /mJ cm^{-2}	SFE /mJ cm^{-2}
1	bare	as spun	no FET	86.4	80.3	11.4	10.3	21.7
2	HMDS	as spun	5.5×10^{-7}	94.7	90.0	7.9	8.1	16.0
3	ODTS	as spun	1.6×10^{-6}	97.4	91.1	7.6	7.7	15.3
4	ODTS	160	3.4×10^{-5}	100.4	90.7	13.0	3.3	16.3

Table S3. OPV performance based on P3HT/Ph-H films.

Run	V_{OC} /V	J_{SC} /mA cm^{-2}	FF	PCE /%
1	0.69	2.52	0.44	0.77
2	0.76	2.47	0.36	0.68
3	0.74	2.43	0.37	0.70
4	0.73	2.40	0.37	0.65
5	0.74	2.42	0.36	0.64
average	0.73 ± 0.01	2.45 ± 0.02	0.38 ± 0.02	0.69 ± 0.02

The fabrication conditions of the active BHJ layer were optimized: the blend composition of a 1:1.5 weight ratio of P3HT:Ph-H, a concentration of 20 mg mL^{-1} in CB for spin-coating, and with thermal annealing at 110 °C for 10 min under N_2.

Table S4. OPV performance based on P3HT/Ph-D films.

Run	V_{OC} /V	J_{SC} /mA cm^{-2}	FF	PCE /%
1	0.49	0.87	0.31	0.13
2	0.51	0.98	0.27	0.14
3	0.51	1.03	0.31	0.16
4	0.51	1.01	0.31	0.16
5	0.51	0.99	0.32	0.16
average	0.51 ± 0.00	0.98 ± 0.03	0.30 ± 0.01	0.15 ± 0.01

The fabrication conditions of the active BHJ layer were optimized: the blend composition of a 1:1 weight ratio of P3HT:Ph-D, a concentration of 20 mg mL^{-1} in *o*-DCB for spin-coating, and without thermal annealing.

Table S5. OPV performance based on P3HT/Ph-EH films.

Run	V_{OC} /V	J_{SC} /mA cm^{-2}	FF	PCE /%
1	0.90	3.80	0.44	1.50
2	0.89	3.99	0.45	1.58
3	0.80	3.26	0.50	1.29
4	0.78	3.81	0.48	1.42
5	0.79	3.23	0.50	1.28
average	0.83 ± 0.03	3.62 ± 0.16	0.47 ± 0.01	1.41 ± 0.06

The fabrication conditions of the active BHJ layer were optimized: the blend composition of a 1:1 weight ratio of P3HT:Ph-EH, a concentration of 20 mg mL^{-1} in CB for spin-coating, and without thermal annealing.

Table S6. OPV performance based on P3HT/Ph-MH films.

Run	V_{OC} /V	J_{SC} /mA cm^{-2}	FF	PCE /%
1	0.76	4.83	0.48	1.79
2	0.76	4.85	0.49	1.79
3	0.76	4.95	0.50	1.88
4	0.75	5.64	0.48	2.04
5	0.76	5.59	0.48	2.05
average	0.76 ± 0.00	5.17 ± 0.18	0.49 ± 0.00	1.91 ± 0.06

The fabrication conditions of the active BHJ layer were optimized: the blend composition of a 1:1 weight ratio of P3HT:Ph-MH, a concentration of 10 mg mL^{-1} in $CHCl_3$ for spin-coating, and without thermal annealing.

Table S7. OPV performance based on P3HT/Ph-Ipop films.

Run	V_{OC} /V	J_{SC} /mA cm^{-2}	FF	PCE /%
1	0.66	0.46	0.27	0.08
2	0.66	0.46	0.29	0.09
3	0.65	0.50	0.29	0.09
4	0.66	0.55	0.29	0.11
5	0.66	0.49	0.29	0.09
average	0.66 ± 0.00	0.49 ± 0.02	0.29 ± 0.00	0.09 ± 0.01

The fabrication conditions of the active BHJ layer were optimized: the blend composition of a 1:1 weight ratio of P3HT:Ph-Ipop, a concentration of 20 mg mL^{-1} in *o*-DCB for spin-coating, and without thermal annealing.

Table S8. OPV performance based on P3HT/Th-EH films.

Run	V_{OC} /V	J_{SC} /mA cm^{-2}	FF	PCE /%
1	0.65	1.62	0.34	0.37
2	0.64	1.37	0.34	0.29
3	0.72	1.44	0.36	0.38
4	0.72	1.37	0.36	0.36
5	0.72	1.36	0.37	0.36
average	0.69 ± 0.02	1.43 ± 0.05	0.35 ± 0.01	0.35 ± 0.02

The fabrication conditions of the active BHJ layer were optimized: the blend composition of a 1:1 weight ratio of P3HT:Th-EH, a concentration of 20 mg mL^{-1} in *o*-DCB for spin-coating, and without thermal annealing.

Table S9. OPV performance based on P3HT/Py-EH films.

Run	V_{OC} /V	J_{SC} /mA cm^{-2}	FF	PCE /%
1	0.56	1.04	0.54	0.32
2	0.47	1.43	0.42	0.28
3	0.47	1.44	0.42	0.28
4	0.46	1.35	0.41	0.26
5	0.45	1.30	0.41	0.24
average	0.48 ± 0.02	1.31 ± 0.07	0.44 ± 0.03	0.28 ± 0.01

The fabrication conditions of the active BHJ layer were optimized: the blend composition of a 1.5:1 weight ratio of P3HT:Py-EH, a concentration of 20 mg mL^{-1} in *o*-DCB for spin-coating, and without thermal annealing.

Table S10. Contact angles and calculated surface free energy data of acceptor films.

Compounds	θ_{water} /°	$\theta_{glycerol}$ /°	γ^d /mJ cm^{-2}	γ^p /mJ cm^{-2}	SFE /mJ cm^{-2}
Ph-H	101.16	90.0	15.1	2.5	17.6
Ph-D	102.84	94.03	11.2	3.2	14.3
Ph-EH	101.1	84.3	25.2	0.7	25.9
Ph-MH	97.6	80.4	27.4	0.1	28.4
Ph-Ipop	82.0	79.5	7.8	15.9	23.7
Th-EH	105.5	96.6	10.6	2.6	13.2
Py-EH	101.3	92.5	11.5	3.5	15.0
P3HT	107.2	102.6	5.4	4.3	9.7
$PC_{61}BM$	84.9	67.1	32.4	3.4	35.8

All the films were prepared on quartz plates.

Experimental Procedures

General Information of Synthesis. Column chromatography was performed on silica gel, KANTO Chemical silica gel 60N (40–50 μm). Thin-layer chromatography plates were visualized with UV light. Preparative gel-permeation chromatography (GPC) was performed on a Japan Analytical Industry LC-918 equipped with JAI-GEL 1H/2H. ^{1}H and ^{13}C NMR spectra were recorded on a JEOL ECS-400 spectrometer in $CDCl_3$ with tetramethylsilane (TMS) as an internal standard. Data are reported as follows: chemical shift in ppm (δ), multiplicity (s = singlet, d = doublet, t = triplet, m = multiplet, br = broad), coupling constant (Hz), and integration. Mass spectra were obtained on a Shimadzu GCMS-QP-5050 or Shimadzu AXIMA-TOF. Elemental analyses were performed on Perkin Elmer LS-50B by the Elemental Analysis Section of CAC, ISIR, Osaka University.

Preparation of Materials. All reactions were carried out under a nitrogen atmosphere. Solvents of the highest purity grade were used as received. Unless stated otherwise, all reagents were purchased from commercial sources and used without purification. 2-bromothieno[2,3-*c*]furan-4,6-dione was prepared by our previously reported procedure.[2] 5-bromo-2-hexylisoindoline-1,3-dione (1a), 6-bromo-2-(2-ethylhexyl)-1*H*-benzo[*de*]isoquinoline-1,3(2*H*)-dione (1g), 3-bromofuro[3,4-*b*]pyridine-5,7-dione, and 4,7-diethynyl-2,1,3-benzothiadiazole (2) were prepared by reported procedures, and ^{1}H NMR data of these compounds were in agreement with those previously reported.[3-6]

Synthesis

Synthesis of 1b: 4-Bromophthalic anhydride (4.00 g, 17.6 mmol) and 1-dodecylamine (3.26 g, 17.6 mmol) were placed in a round-bottomed flask and dissolved with DMF (100 mL). The reaction mixture was stirred at 140 °C for 12 h. After being cooled to room temperature and addition of water, the resulting mixture was extracted with ethyl acetate (EtOAc) and the organic layer was washed with water. After removal of the solvent under reduced pressure, the residue was purified by column chromatography on silica gel (hexane/EtOAc = 10/1) to give 1b (4.74 g, 68%). Colorless solid; m.p.: 63-64 °C; ^{1}H NMR (400 MHz, $CDCl_3$, TMS, δ): 7.97 (d, J = 1.4 Hz, 1H), 7.85 (dd, J = 8.0, 1.6 Hz, 1H), 7.70 (d, J = 8.0 Hz, 1H), 3.66 (t, J = 7.3 Hz, 2H), 1.65 (m, 2H), 1.35-1.23 (br, 16H), 0.88 (t, J = 6.6 Hz, 3H); ^{13}C NMR (100 MHz, $CDCl_3$, δ): 167.54, 166.99, 136.79, 133.81, 130.69, 128.71, 126.51, 124.51, 38.30, 31.91, 29.62, 29.62, 29.59, 29.49, 29.35, 29.18, 28.52, 26.84, 22.69, 14.14; MS (GC) *m/z* 393 (M^+, Calcd 393.13). Anal. calcd for $C_{20}H_{28}BrNO_2$: C 60.91, H 7.16, N 3.55; found: C 60.82, H 7.06, N 3.42.

Synthesis of 1c: 4-Bromophthalic anhydride (5.00 g, 22.0 mmol) and 2-aminoheptane (2.50 g, 22.0 mmol) were placed in a round-bottomed flask and dissolved with DMF (100 mL). The reaction mixture was stirred at 145 °C for 12 h. After being cooled to room temperature and addition of water, the resulting mixture was extracted with EtOAc and the organic layer was washed with water. After removal of the solvent under reduced pressure, the residue was purified by column chromatography on silica gel (hexane/EtOAc = 4/1) to give 1c (3.60 g, 50%). Colorless solid; m.p.: 84-85 °C; ^{1}H NMR (400 MHz, $CDCl_3$, TMS, δ): 7.95 (d, J = 1.8 Hz, 1H), 7.84 (dd, J = 7.8, 1.8 Hz, 1H), 7.68 (d, J = 7.8 Hz, 1H), 4.32 (m, 1H), 2.02 (m, 1H), 1.71 (m, 1H), 1.45 (d, J = 7.3 Hz, 3H) , 1.30-1.15 (br, 6H), 0.84 (t, J = 6.8 Hz, 3H); ^{13}C NMR (100 MHz, $CDCl_3$, δ): 167.69, 167.12, 136.75, 133.65, 130.51, 128.65, 126.42, 124.43, 47.78, 33.59, 31.37, 26.42, 22.49, 18.64, 13.99; MS (GC) *m/z* 323 (M^+, Calcd 323.05). Anal. calcd for $C_{15}H_{18}BrNO_2$: C 55.57, H 5.60, N 4.32; found: C 55.50, H 5.33, N 4.34.

Synthesis of 1d: 4-Bromophthalic anhydride (4.00 g, 17.6 mmol) and 3-isopropoxypropylamine (2.06 g, 17.6 mmol) were placed in a round-bottomed flask and dissolved with DMF (50 mL). The reaction mixture was stirred at 140 °C for 24 h. After being cooled to room temperature and addition of water, the resulting mixture was extracted with EtOAc and the organic layer was washed with water. After removal of the solvent under reduced pressure, the residue was purified by column chromatography on silica gel (hexane/EtOAc = 10/1) to give 1d (3.50 g, 61%). Colorless solid; m.p.: 74-75 °C; ^{1}H NMR (400 MHz, $CDCl_3$, TMS, δ): 7.97 (d, J = 1.5 Hz, 1H), 7.84 (dd, J = 8.0, 1.5 Hz, 1H), 7.70 (d, J = 8.0 Hz, 1H), 3.80 (d, J = 6.9 Hz, 2H), 3.49 (m, 1H), 3.45 (t, J = 6.0 Hz, 2H), 1.93 (m, 2H), 1.06 (d, J = 6.4 Hz, 6H); ^{13}C NMR (100 MHz, $CDCl_3$, δ): 167.59, 167.05, 136.78, 133.89, 130.78, 128.66, 126.50, 124.49, 71.56, 65.61, 36.08, 28.81, 21.94; MS (GC) *m/z* 325 (M^+, Calcd 325.03). Anal. calcd for $C_{14}H_{16}BrNO_3$: C 51.55, H 4.94, N 4.29; found: C 51.42, H 5.03, N 4.36.

Synthesis of 1e: 2-Bromothieno[2,3-*c*]furan-4,6-dione (1.00 g, 4.29 mmol) and 2-ethyl-1-hexylamine (555 mg, 4.29 mmol) were placed in a round-bottomed flask and dissolved with toluene (40 mL), and the resulting mixture was

refluxed for 20 h. After being cooled to room temperature, the solvent was removed under reduced pressure and $SOCl_2$ (50 mL) was added. The resulting mixture was refluxed for 3 h. After removal of the solvent under reduced pressure, the residue was purified by column chromatography on silica gel (hexane/EtOAc = 19/1) to give 1e (770 mg, 52%). Colorless solid; m.p.: 61-62 °C; ^{1}H NMR (400 MHz, $CDCl_3$, TMS, δ): 7.31 (s, 1H), 3.48 (d, J = 7.3 Hz, 2H), 1.76 (m, 1H), 1.35-1.25 (br, 8H), 0.90 (t, J = 7.3 Hz, 3H), 0.88 (t, J = 6.9 Hz, 3H); ^{13}C NMR (100 MHz, $CDCl_3$, δ): 163.26, 162.24, 143.78, 140.38, 125.42, 123.83, 42.47, 38.34, 30.39, 28.43, 23.71, 23.01, 14.07, 10.39; MS (GC) *m/z* 343 (M^+, Calcd 343.02). Anal. calcd for $C_{14}H_{18}BrNO_2S$: C 48.84, H 5.27, N 4.07; found: C 49.32, H 5.09, N 4.09.

Synthesis of 1f: 3-Bromofuro[3,4-*b*]pyridine-5,7-dione (460 mg, 2.01 mmol) and 2-ethyl-1-hexylamine (340 mg, 2.62 mmol) were placed in a round-bottomed flask and dissolved with AcOH (4 mL). The reaction mixture was refluxed for 12 h. After being cooled to room temperature and addition of water, the resulting mixture was extracted with toluene and the organic layer was washed with water. After removal of the solvent under reduced pressure, the residue was purified by column chromatography on silica gel (hexane/$CHCl_3$ = 1/1) to give 1f (288 mg, 42%). Colorless solid; m.p.: 97-98 °C; ^{1}H NMR (400 MHz, $CDCl_3$, TMS, δ): 9.02 (d, J = 2.0 Hz, 1H), 8.28 (d, J = 2.0 Hz, 1H), 3.64 (d, J = 7.3 Hz, 2H), 1.85 (m, 1H), 1.40-1.24 (br, 8H), 0.91 (t, J = 7.3 Hz, 3H), 0.88 (t, J = 7.0 Hz, 3H); ^{13}C NMR (100 MHz, $CDCl_3$, δ): 165.82, 165.17, 156.31, 149.64, 133.73, 128.42, 125.44, 42.40, 38.21, 30.41, 28.38, 23.75, 22.98, 14.05, 10.35; MS (GC) *m/z* 337 (M^+, Calcd 338.06). Anal. calcd for $C_{15}H_{19}BrN_2O_2$: C 53.11, H 5.65, N 8.26; found: C 53.11, H 5.54, N 8.21.

Synthesis of Ph-H: 1a (194 mg, 0.63 mmol), 2 (48 mg, 0.26 mmol), CuI (5 mg, 0.03 mmol), and $Pd(PPh_3)_4$ (30 mg, 0.03 mmol) were placed in a test tube with screw cap and dissolved with toluene (6 mL) and triethylamine (3 mL). The reaction mixure was refluxed for 1.5 h. After being cooled to room temperature, the reaction mixture was concentrated under reduced pressure and then purified by column chromatography on silica gel ($CHCl_3$), followed by purification with preparative GPC ($CHCl_3$) to give Ph-H (102 mg, 61%). Yellow solid; m.p.: 200-201 °C; ^{1}H NMR (400 MHz, $CDCl_3$, TMS, δ): 8.11 (s, 2H), 7.99 (d, J = 7.8, 2H), 7.88 (d, J = 7.8 Hz, 2H), 7.87 (s, 2H), 3.70 (t, J = 7.3 Hz, 4H), 1.69 (m, 4H), 1.40-1.27 (br, 12H), 0.89 (t, 6H); ^{13}C NMR (100 MHz, $CDCl_3$, δ): 167.69, 167.59, 154.17, 137.17, 132.91, 132.51, 131.69, 128.36, 126.41, 123.28, 117.03, 95.83, 88.94, 38.33, 31.36, 28.54, 26.54, 22.52, 14.03; MS MALDI-TOF (1,8,9-trihydroxyanthracene matrix) *m/z* 642.41 (M^+, Calcd 642.23); Anal. calcd for $C_{38}H_{34}N_4O_4S$: C 71.01, H 5.33, N 8.72; found: C 71.03, H 5.45, N 8.72.

Synthesis of Ph-D: Ph-D was synthesized from compound 1b (529 mg, 1.34 mmol), 2 (103 mg, 0.56 mmol), CuI (11 mg, 0.06 mmol), and $Pd(PPh_3)_4$ (65 mg, 0.06 mmol) with a yield of 59% by following the procedure used for the preparation of Ph-H. Yellow solid; m.p.: 175-176 °C; ^{1}H NMR (400 MHz, $CDCl_3$, TMS, δ): 8.11 (s, 2H), 7.99 (dd, J = 7.8, 1.4 Hz, 2H), 7.88 (d, J = 7.8 Hz, 2H), 7.87 (s, 2H), 3.70 (t, J = 7.6 Hz, 4H), 1.69 (m, 4H), 1.35-1.25 (br, 36H), 0.88 (t, J = 7.0 Hz, 6H); ^{13}C NMR (100 MHz, $CDCl_3$, δ): 167.70, 167.59, 154.17, 137.17, 132.91, 132.52, 131.69, 128.36, 123.28, 117.04, 95.84, 88.94, 38.34, 31.92, 29.62, 29.62, 29.57, 29.50, 29.35, 29.19, 28.58, 26.89, 22.69, 14.14; MS

MALDI-TOF (1,8,9-trihydroxyanthracene matrix) *m/z* 810.77 (M^+, Calcd 810.42). Anal. calcd for $C_{50}H_{58}N_4O_4S$: C 74.04, H 7.21, N 6.91; found: C 74.03, H 7.21, N 6.79.

Synthesis of Ph-MH: Ph-MH was synthesized from compound 1c (414 mg, 1.28 mmol), 2 (98 mg, 0.53 mmol), CuI (10 mg, 0.05 mmol), and $Pd(PPh_3)_4$ (61 mg, 0.05 mmol) with a yield of 60% by following the procedure used for the preparation of Ph-H. Yellow solid; m.p.: 203-204 °C; ^{1}H NMR (400 MHz, $CDCl_3$, TMS, δ): 8.09 (s, 2H), 7.98 (d, J = 7.6 Hz, 2H), 7.88 (s, 2H), 7.86 (d, J = 7.6 Hz, 2H), 4.36 (m, 2H), 2.06 (m, 2H), 1.75 (m, 2H), 1.49 (d, J = 6.9 Hz, 6H), 1.28 (br, 12H), 0.86 (t, J = 6.9 Hz, 6H); ^{13}C NMR (100 MHz, $CDCl_3$, δ): 167.81, 167.68, 154.17, 137.14, 132.91, 132.34, 131.54, 128.30, 126.30, 123.17, 117.04, 95.88, 88.86, 47.79, 33.65, 31.41, 26.47, 22.51, 18.67, 14.01; MS MALDI-TOF (1,8,9-trihydroxyanthracene matrix) *m/z* 670.52 (M^+, Calcd 670.26). Anal. calcd for $C_{40}H_{38}N_4O_4S$: C 71.62, H 5.71, N 8.35; found: C 71.60, H 5.74, N 8.24.

Synthesis of Ph-Ipop: Ph-Ipop was synthesized from compound 1d (217 mg, 0.66 mmol), 2 (51 mg, 0.28 mmol), CuI (5 mg, 0.03 mmol), and $Pd(PPh_3)_4$ (32 mg, 0.03 mmol) with a yield of 55% by following the procedure used for the preparation of Ph-H. Yellow solid; m.p.: 219-220 °C; ^{1}H NMR (400 MHz, $CDCl_3$, TMS, δ): 8.11 (s, 2H), 7.99 (d, J = 7.8, 2H), 7.88 (d, J = 7.8 Hz, 2H), 7.87 (s, 2H), 3.83 (t, J = 6.6 Hz, 4H), 3.51 (m, 2H), 3.48 (t, J = 6.0 Hz, 4H), 1.96 (m, 4H), 1.08 (d, J = 6.0 Hz, 12H); ^{13}C NMR (100 MHz, $CDCl_3$, δ): 167.71, 167.56, 154.18, 137.15, 132.92, 132.62, 131.82, 128.32, 126.37, 123.25, 117.04, 95.85, 88.90, 71.58, 65.68, 36.12, 28.87, 21.97; MS MALDI-TOF (1,8,9-trihydroxyanthracene matrix) *m/z* 674.50 (M^+, Calcd 674.22). Anal. calcd for $C_{38}H_{34}N_4O_6S$: C 67.64, H 5.08, N 8.30; found: C 67.60, H 5.18, N 8.26.

Synthesis of Th-EH: Th-EH was synthesized from compound 1e (351 mg, 1.02 mmol), 2 (85 mg, 0.46 mmol), CuI (8 mg, 0.05 mmol), and $Pd(PPh_3)_4$ (54 mg, 0.05 mmol) in THF (8 mL) and diisopropylethylamine (0.8 mL) with a yield of 91% by following the procedure used for the preparation of Ph-H. Yellow solid; m.p.: 254-255 °C; ^{1}H NMR (400 MHz, $CDCl_3$, TMS, δ): 7.87 (s, 2H), 7.57 (s, 2H), 3.53 (d, J = 6.9 Hz, 4H), 1.80 (m, 2H), 1.37-1.25 (m, 16H), 0.92 (t, J = 7.2 Hz, 6H), 0.89 (t, J = 7.2 Hz, 6H); ^{13}C NMR (100 MHz, $CDCl_3$, δ): 163.66, 162.57, 153.79, 143.82, 141.11, 134.37, 132.85, 125.95, 116.69, 93.35, 89.21, 42,60, 38.41, 30.43, 28.48, 23.77, 23.02, 14.07, 10.41; MS MALDI-TOF (1,8,9-trihydroxyanthracene matrix) *m/z* 710.40 (M^+, Calcd 710.21). Anal. calcd for $C_{38}H_{38}N_4O_4S_3$: C 64.20, H 5.39, N 7.88; found: C 64.24, H 5.47, N 7.70.

Synthesis of Py-EH: Py-EH was synthesized from compound 1f (288 mg, 0.85 mmol), 2 (71 mg, 0.39 mmol), CuI (7 mg, 0.04 mmol), and $Pd(PPh_3)_4$ (45 mg, 0.04 mmol) THF (8 mL) and diisopropylethylamine (0.8 mL) with a yield of 63% by following the procedure used for the preparation of Ph-H. Orange solid; m.p.: 232-233 °C; ^{1}H NMR (400 MHz, $CDCl_3$, TMS, δ): 9.20 (d, J = 1.8 Hz, 2H), 8.38 (d, J = 1.8, 2H), 7.93 (s, 2H), 3.68 (d, J = 6.9 Hz, 4H), 1.88 (m, 1H), 1.40-1.26 (br, 8H), 0.94 (t, J = 7.6, 6H), 0.90 (t, J = 7.0, 6H); ^{13}C NMR (100 MHz, $CDCl_3$, δ): 165.91, 165.71, 157.54,

154.02, 150.18, 133.46, 133.20, 126.90, 123.71, 116.90, 92.90, 91.73, 42.43, 38.26, 30.45, 28.41, 23.79, 23.00, 14.06, 10.37; MS MALDI-TOF (1,8,9-trihydroxyanthracene matrix) *m/z* 700.41 (M^+, Calcd 700.28). Anal. calcd for $C_{40}H_{40}N_6O_2S$: C 68.55, H 5.75, N 11.99; found: C 68.55, H 5.74, N 11.88.

Synthesis of Na-EH: Na-EH was synthesized from compound 1g (306 mg, 0.92 mmol), 2 (123 mg, 0.41 mmol), CuI (8 mg, 0.04 mmol), and $Pd(PPh_3)_4$ (48 mg, 0.04 mmol) THF (8 mL) and diisopropylethylamine (0.8 mL) with a yield of 98% by following the procedure used for the preparation of Ph-H. This compound was purified by column chromatography on silica gel ($CHCl_3$), followed by precipitation using $CHCl_3$ and acetone. Orange solid; m.p.: 281-282 °C; ^{1}H NMR (400 MHz, $CDCl_3$, TMS, δ): 9.03 (d, J = 8.0 Hz, 2H), 8.68 (d, J = 7.3 Hz, 2H), 8.55 (d, J = 8.0 Hz, 2H), 8.08 (d, J = 7.3 Hz, 2H), 7.97 (s, 2H), 7.93 (t, J = 7.3 Hz, 2H), 4.14 (m, 4H), 1.97 (m, 2H), 1.45-1.30 (br, 16H), 0.95 (t, J = 7.6 Hz, 6H), 0.88 (t, J = 7.1 Hz, 6H); ^{13}C NMR (100 MHz, $CDCl_3$, δ): 164.31, 164.06, 154.66, 132.70, 132.48, 132.00, 131.85, 131.32, 130.30, 128.29, 128.02, 126.48, 123.33, 123.28, 117.49, 94.99, 94.27, 44.47, 38.14, 30.98, 28.83, 24.29, 23.11, 14.04, 10.73; MS MALDI-TOF (1,8,9-trihydroxyanthracene matrix) *m/z* 798.55 (M^+, Calcd 798.32). Anal. calcd for $C_{50}H_{46}N_4O_4S$: C 75.16, H 5.80, N 7.01; found: C 75.01, H 5.90, N 6.80.

NMR Spectra

^{1}H NMR spectrum of **1b**.

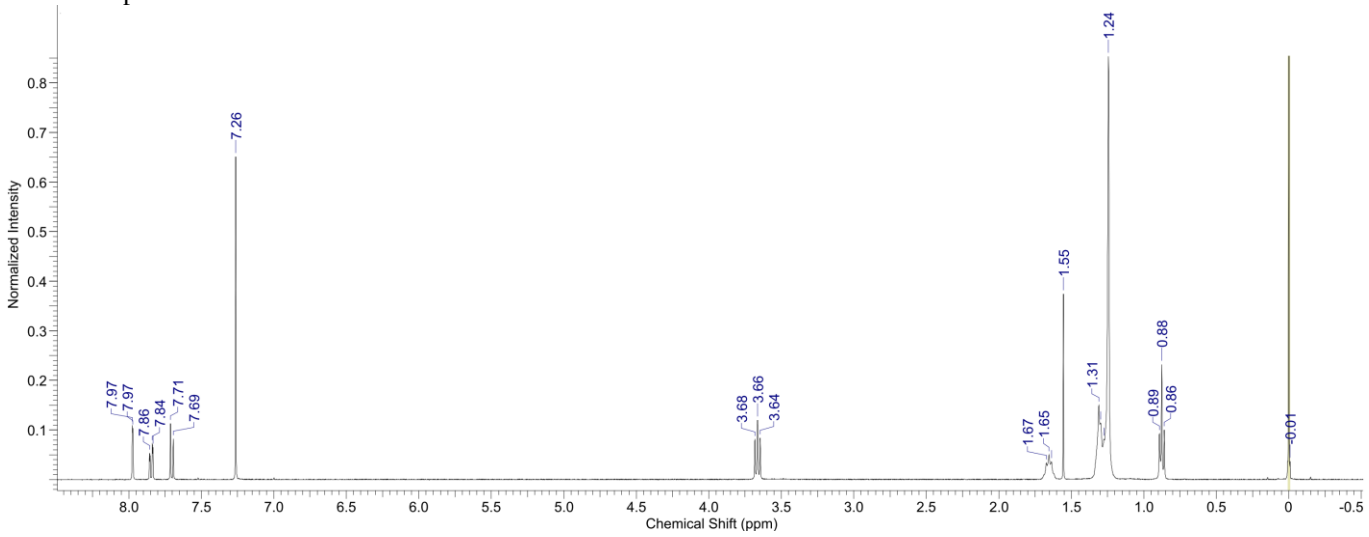

^{13}C NMR spectrum of **1b**.

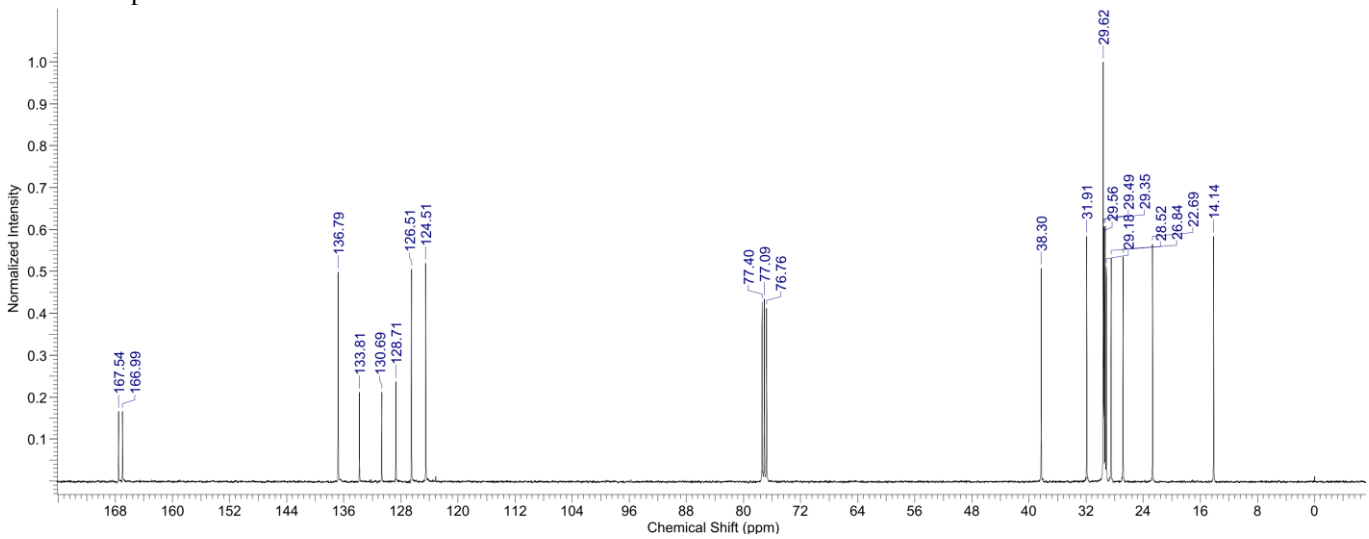

^{1}H NMR spectrum of **1c**.

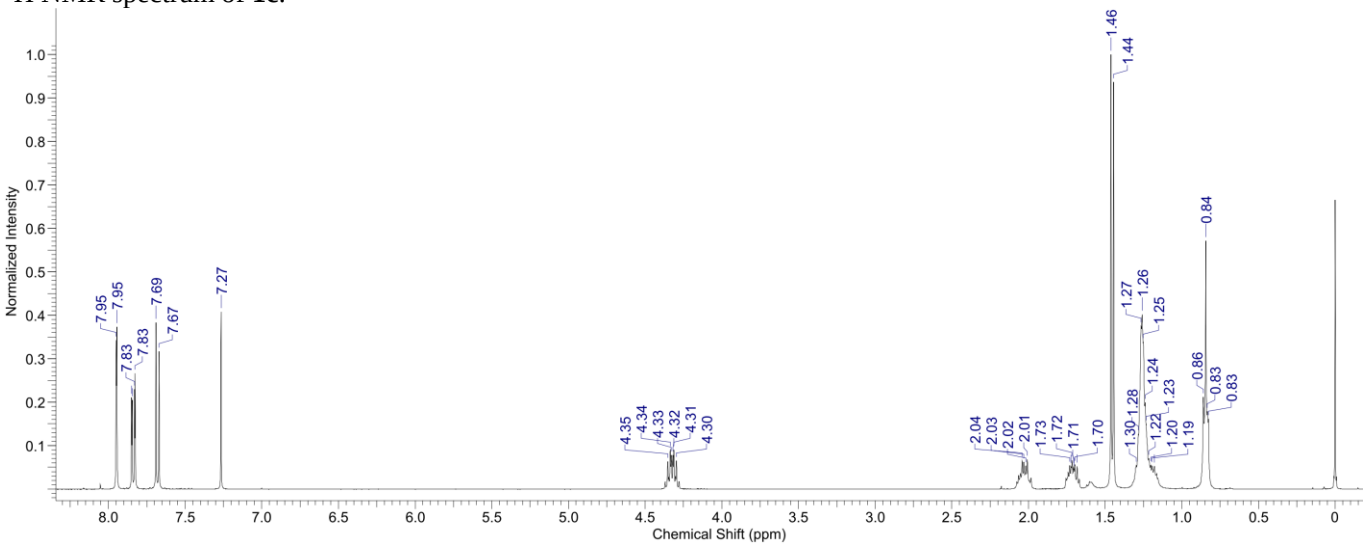

^{13}C NMR spectrum of **1c**.

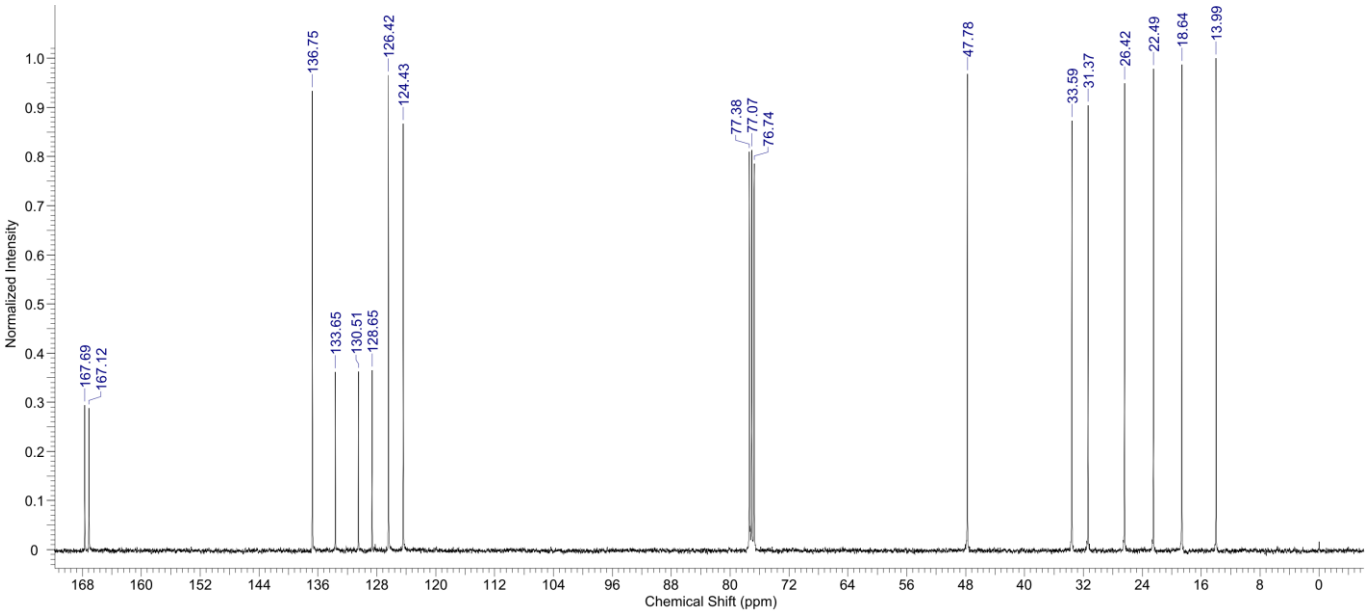

^{1}H NMR spectrum of **1d**.

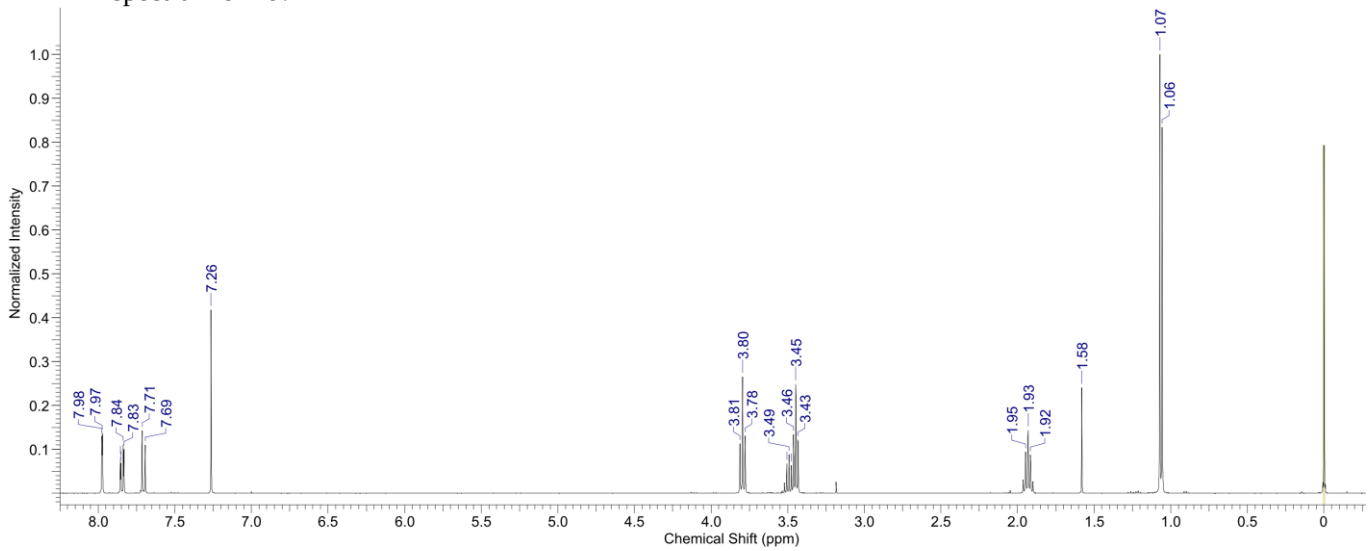

^{13}C NMR spectrum of **1d**.

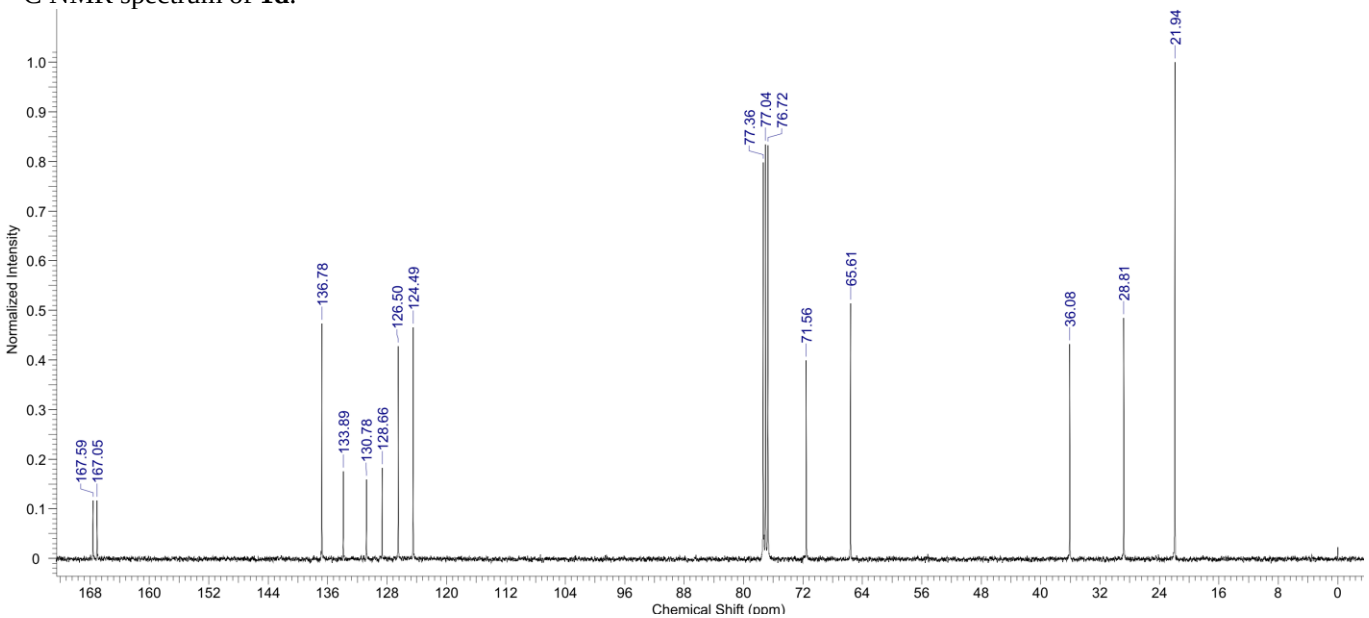

^{1}H NMR spectrum of **1e**.

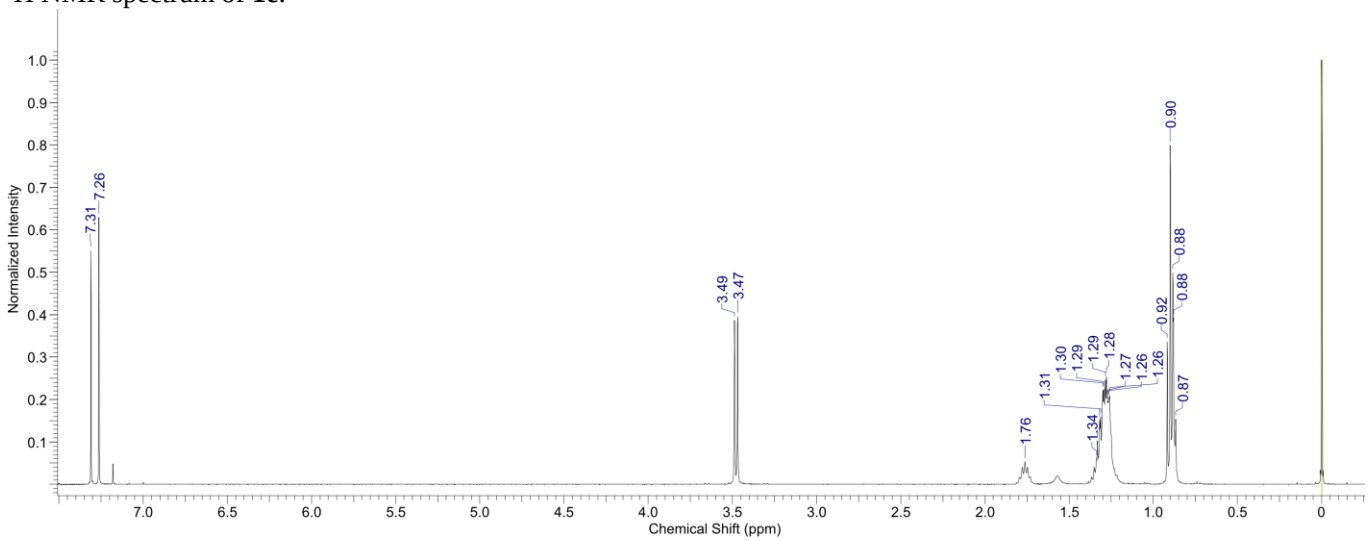

^{13}C NMR spectrum of **1e**.

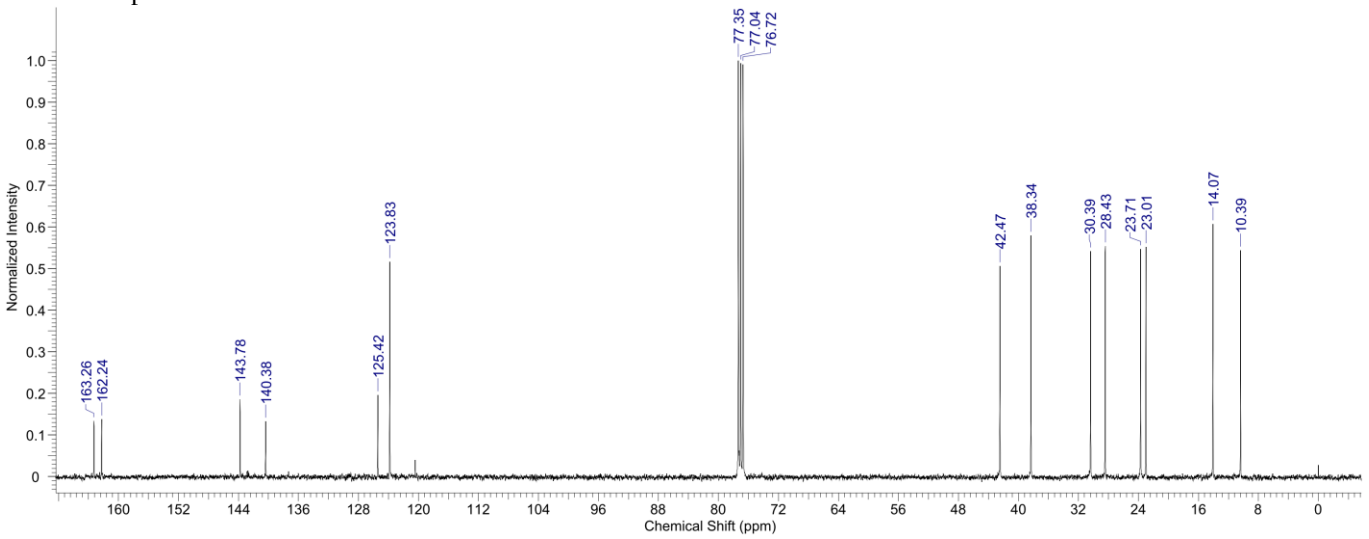

^{1}H NMR spectrum of **1f**.

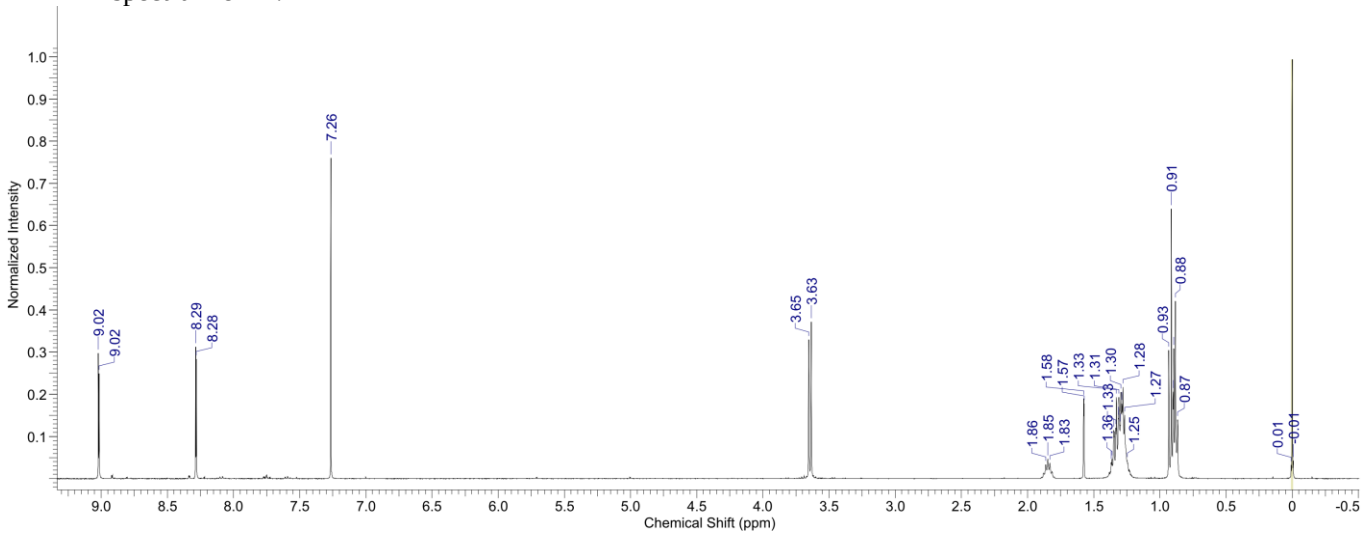

^{13}C NMR spectrum of **1f**.

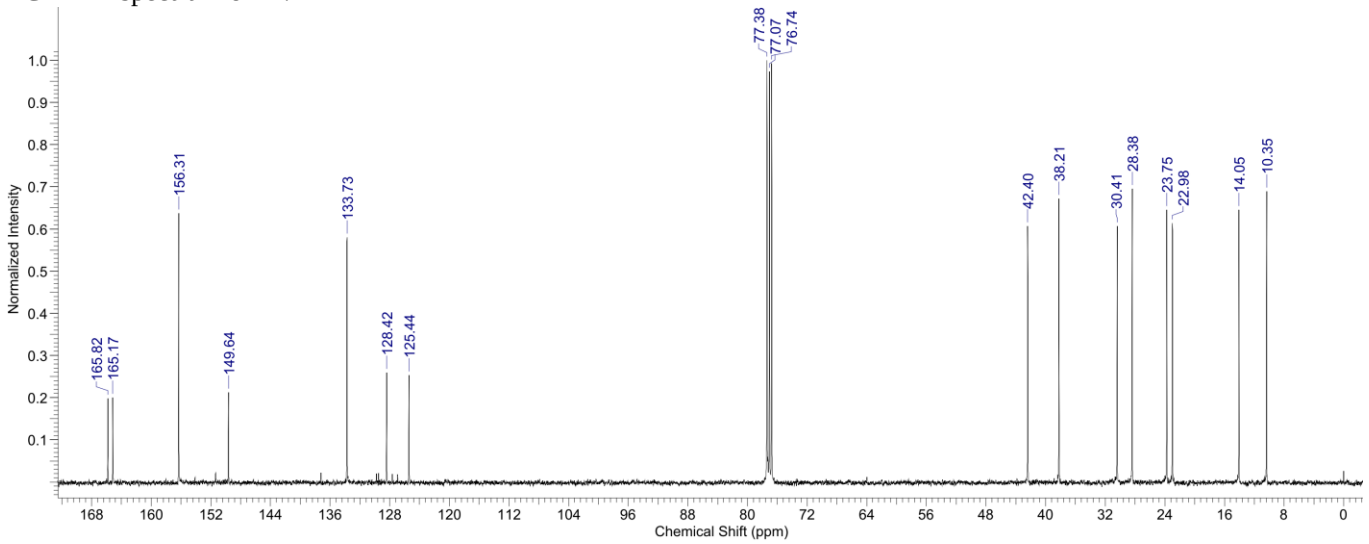

^{1}H NMR spectrum of **Ph-H**.

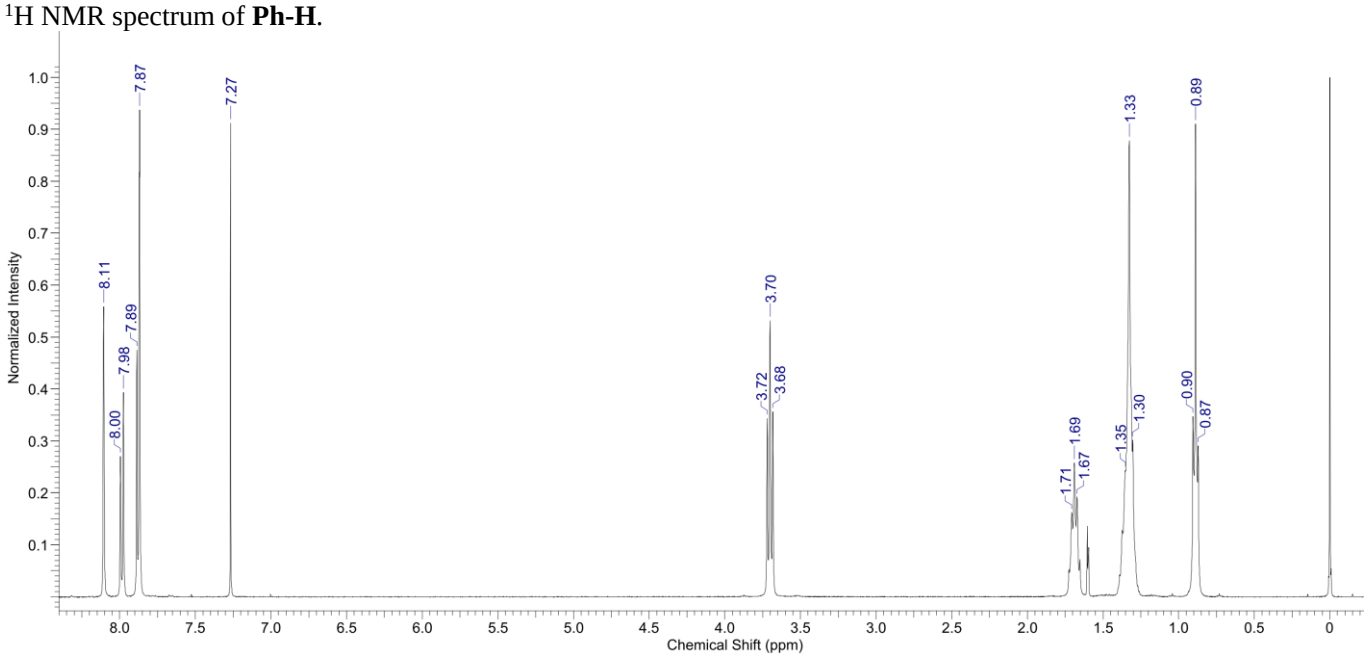

^{13}C NMR spectrum of **Ph-H**.

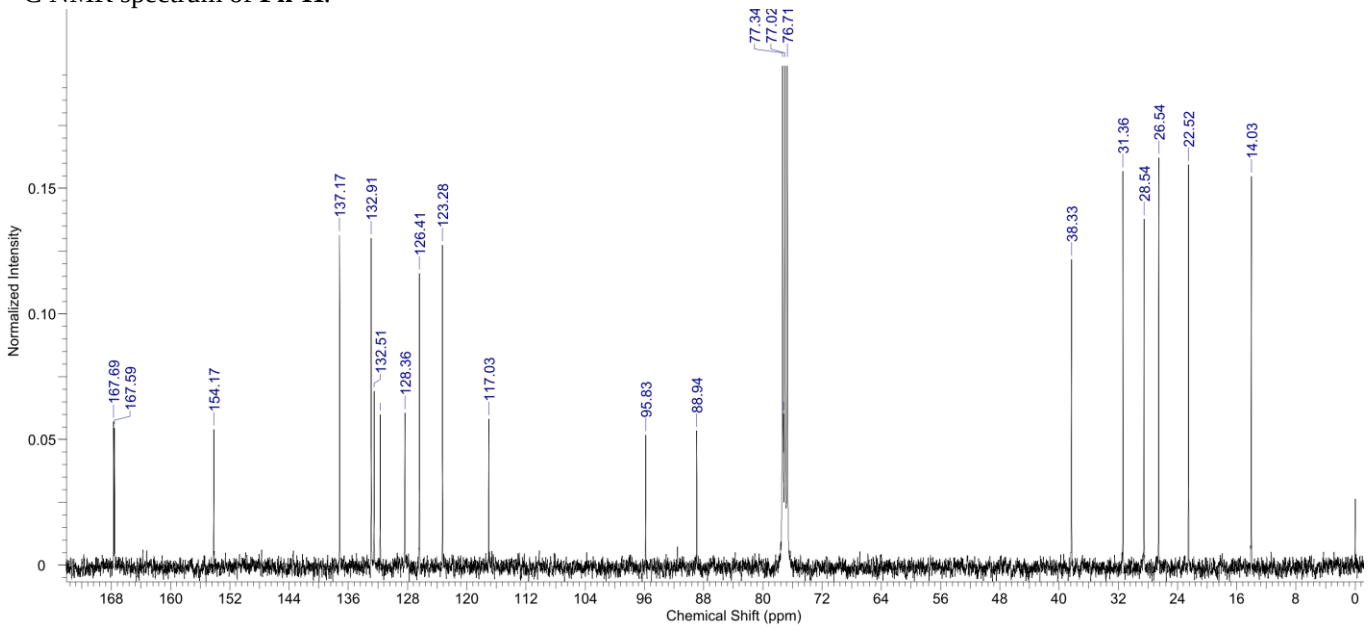

^{1}H NMR spectrum of **Ph-D**.

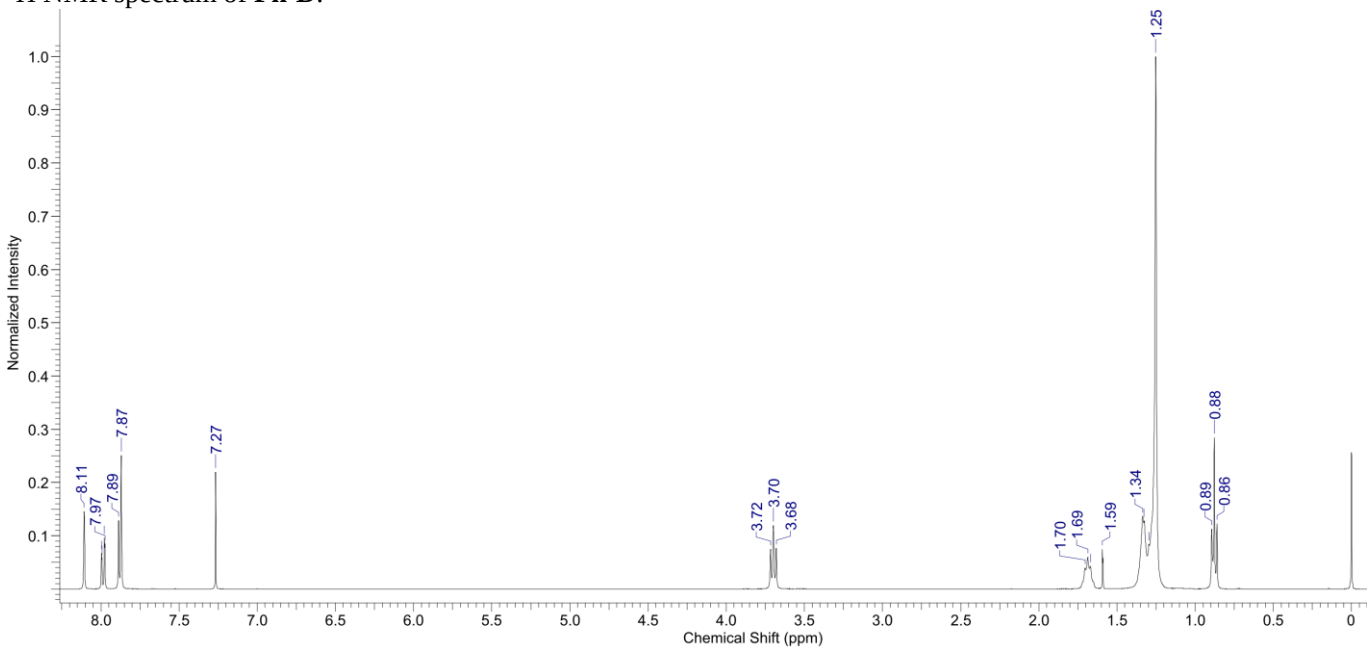

^{13}C NMR spectrum of **Ph-D**.

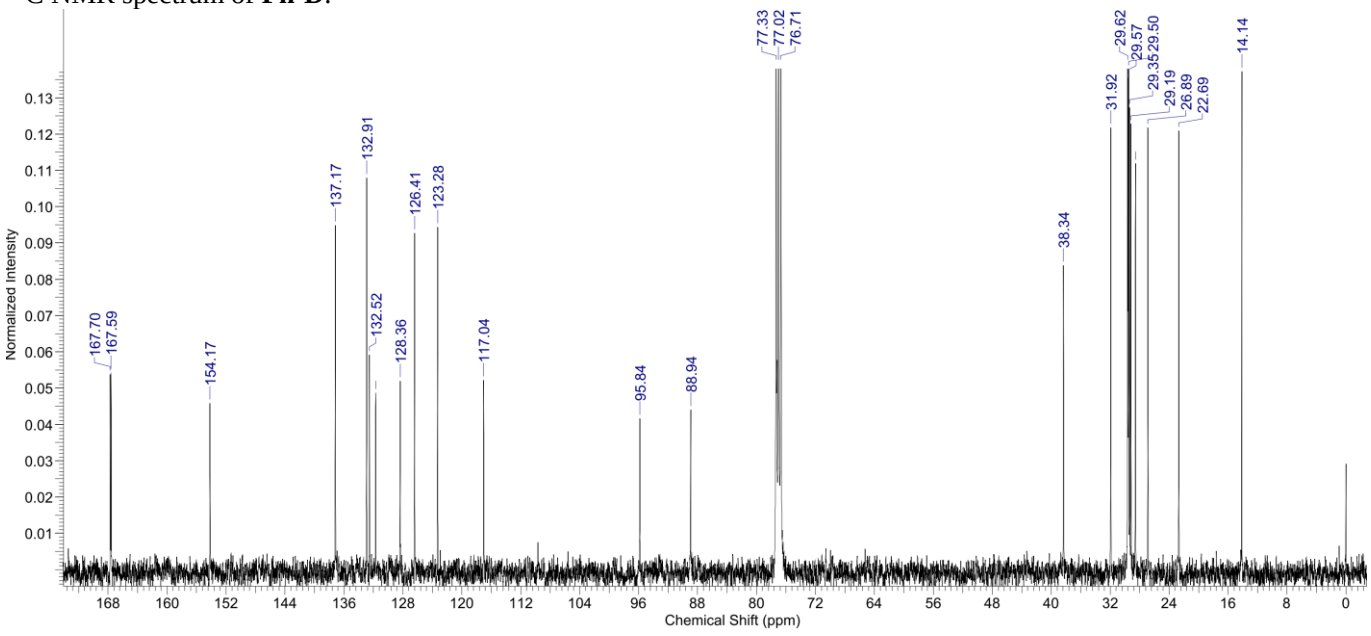

^{1}H NMR spectrum of **Ph-MH**.

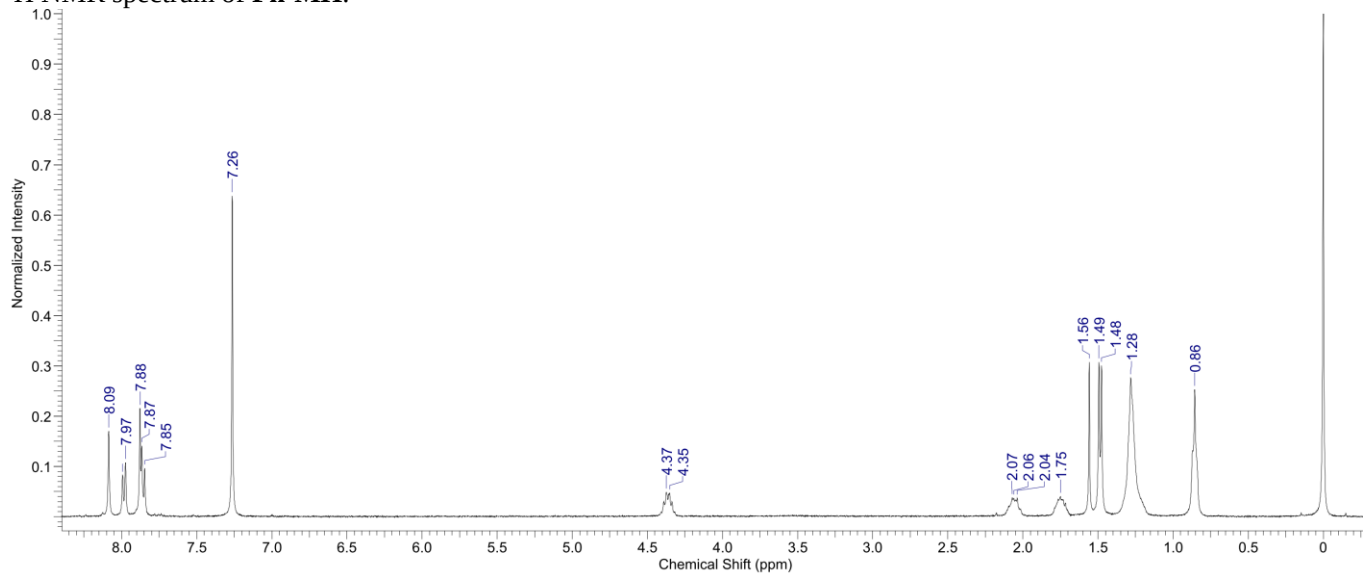

^{13}C NMR spectrum of **Ph-MH**.

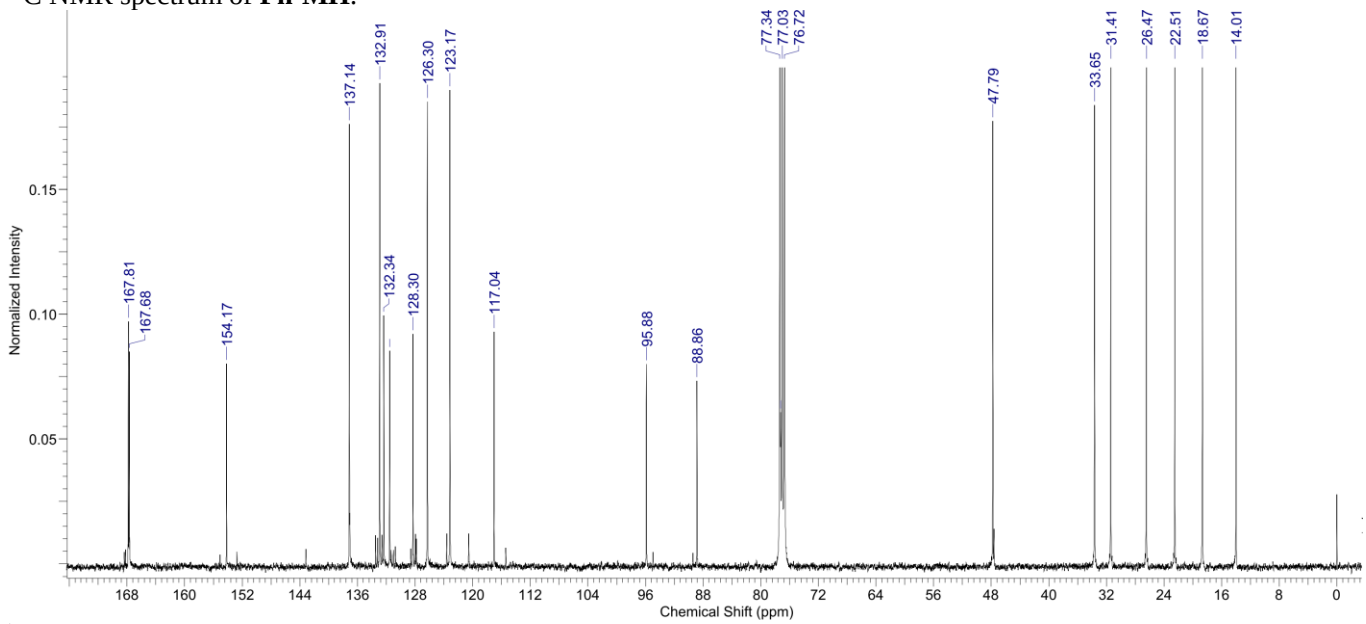

^{1}H NMR spectrum of **Ph-Ipop**.

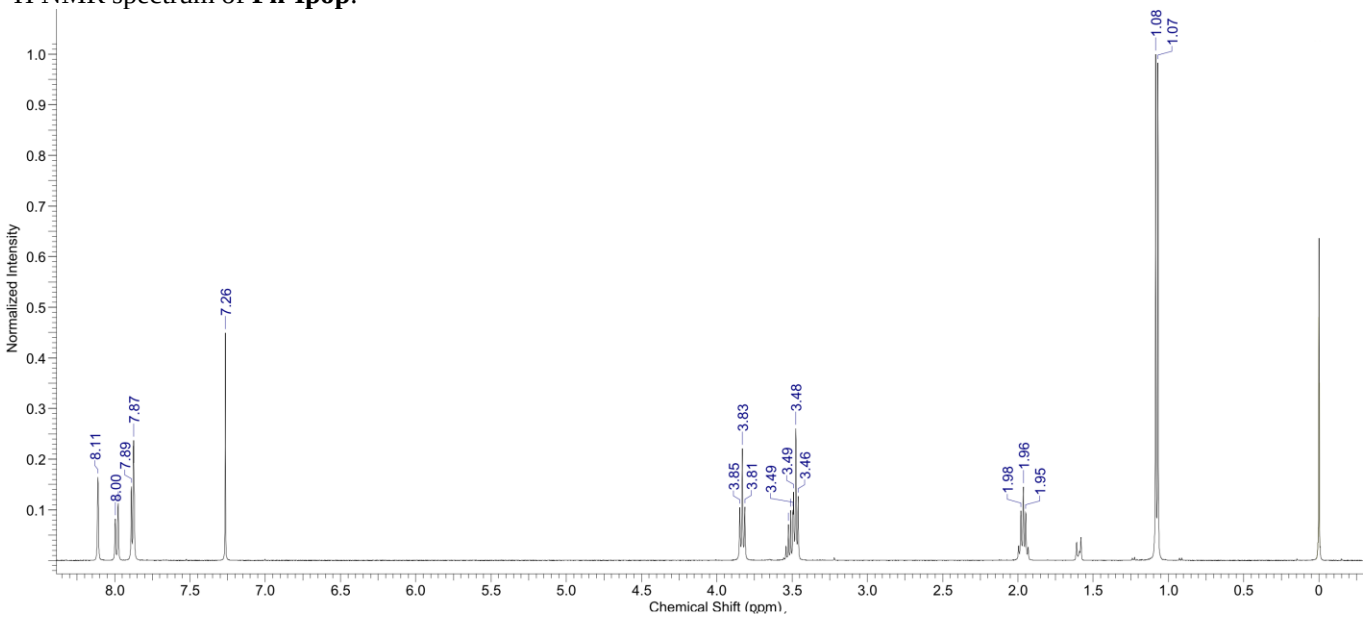

^{13}C NMR spectrum of **Ph-Ipop**.

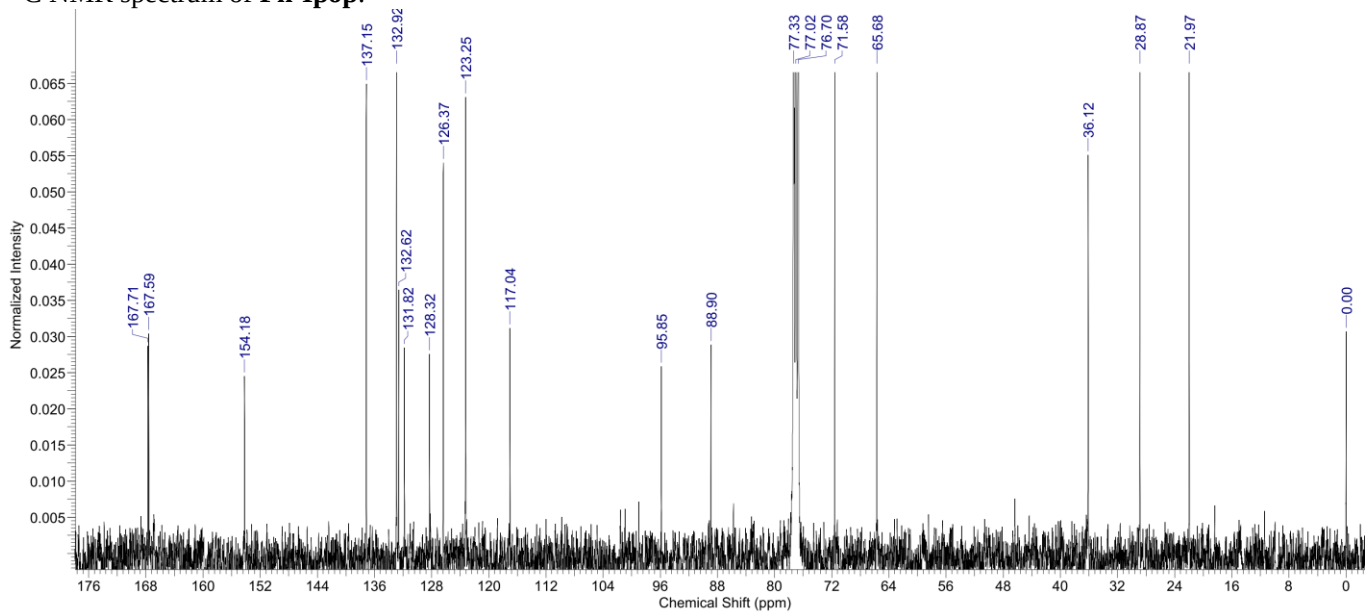

^{1}H NMR spectrum of **Th-EH**.

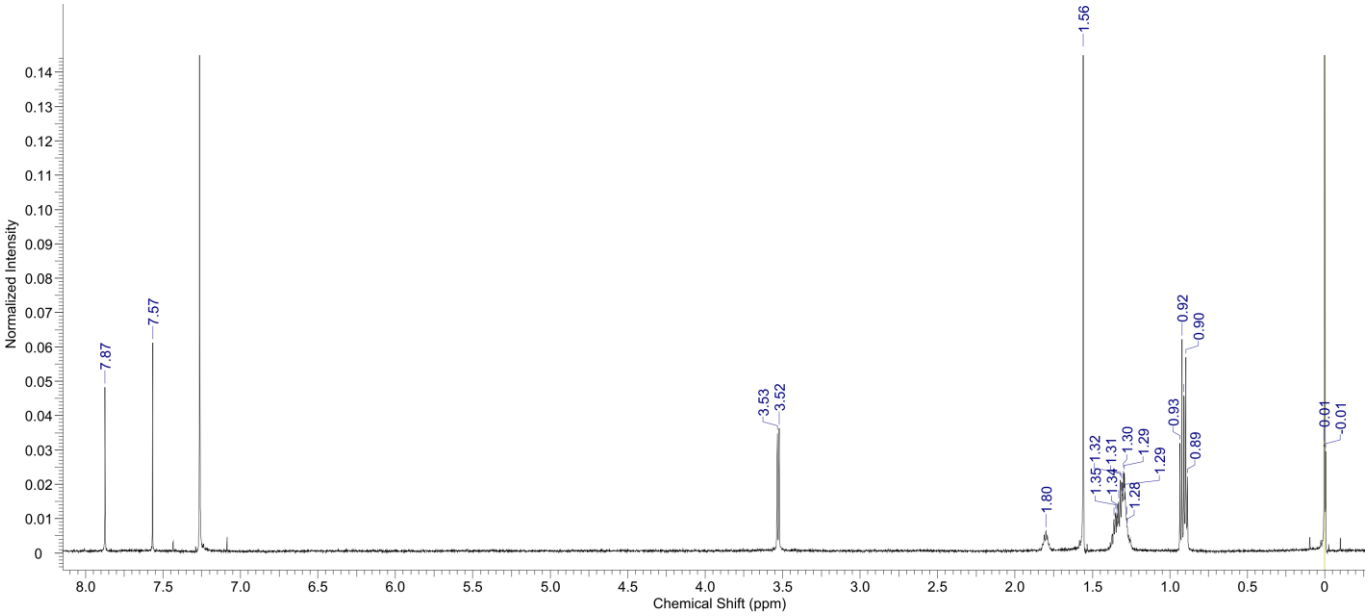

^{13}C NMR spectrum of **Th-EH**.

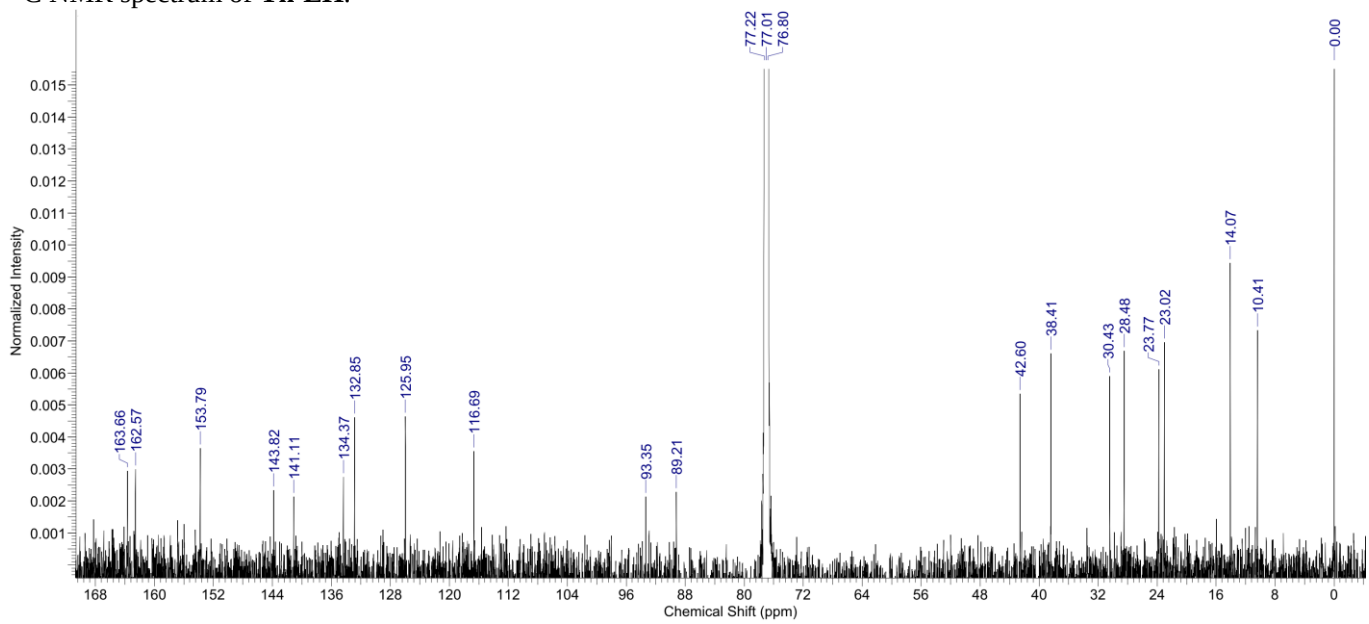

^{1}H NMR spectrum of **Py-EH**.

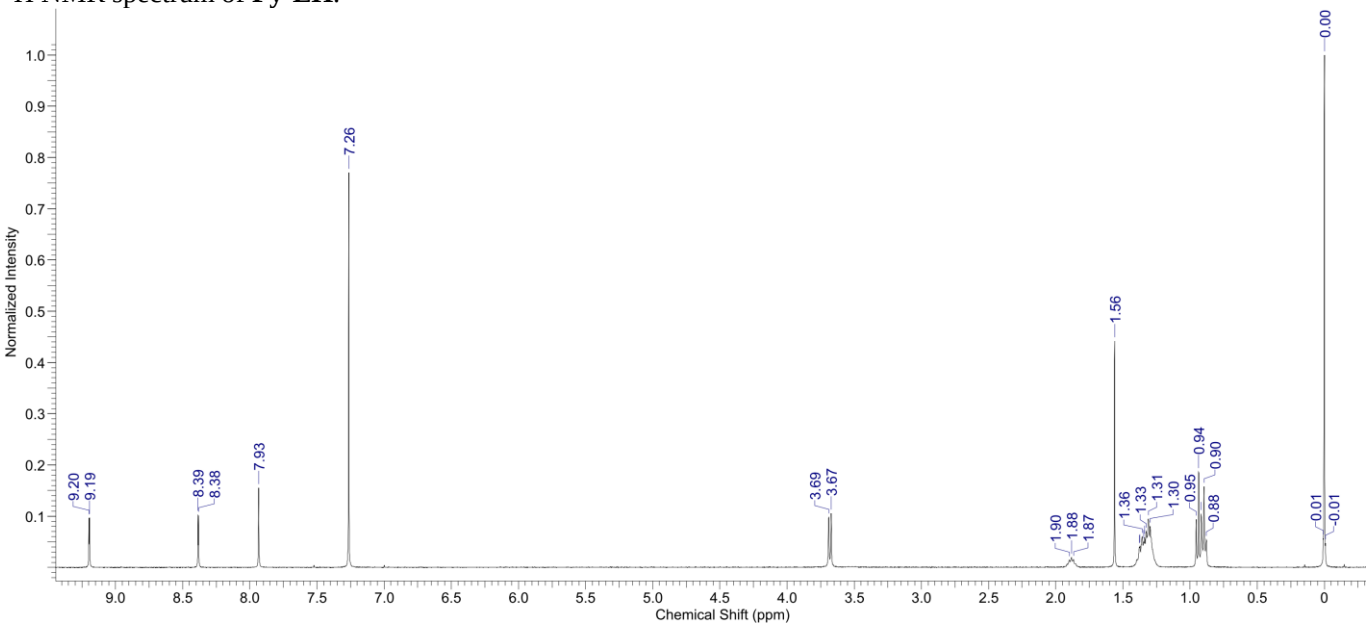

^{13}C NMR spectrum of **Py-EH**.

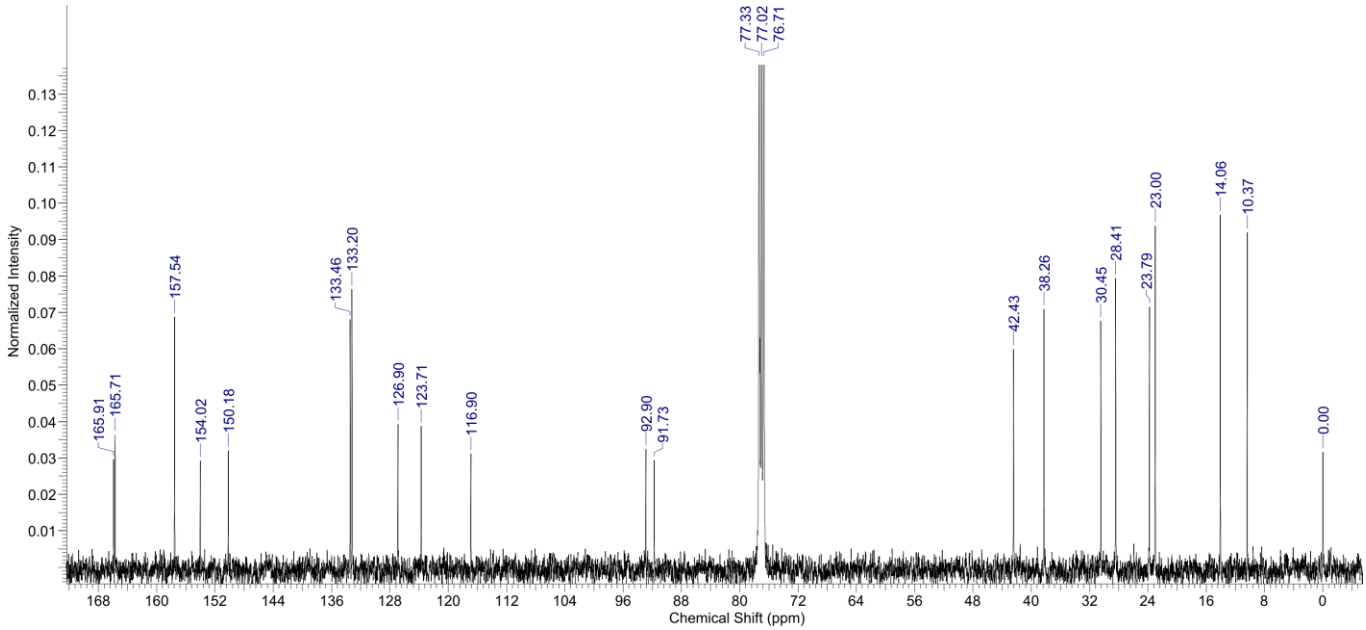

^{1}H NMR spectrum of **Na-EH**.

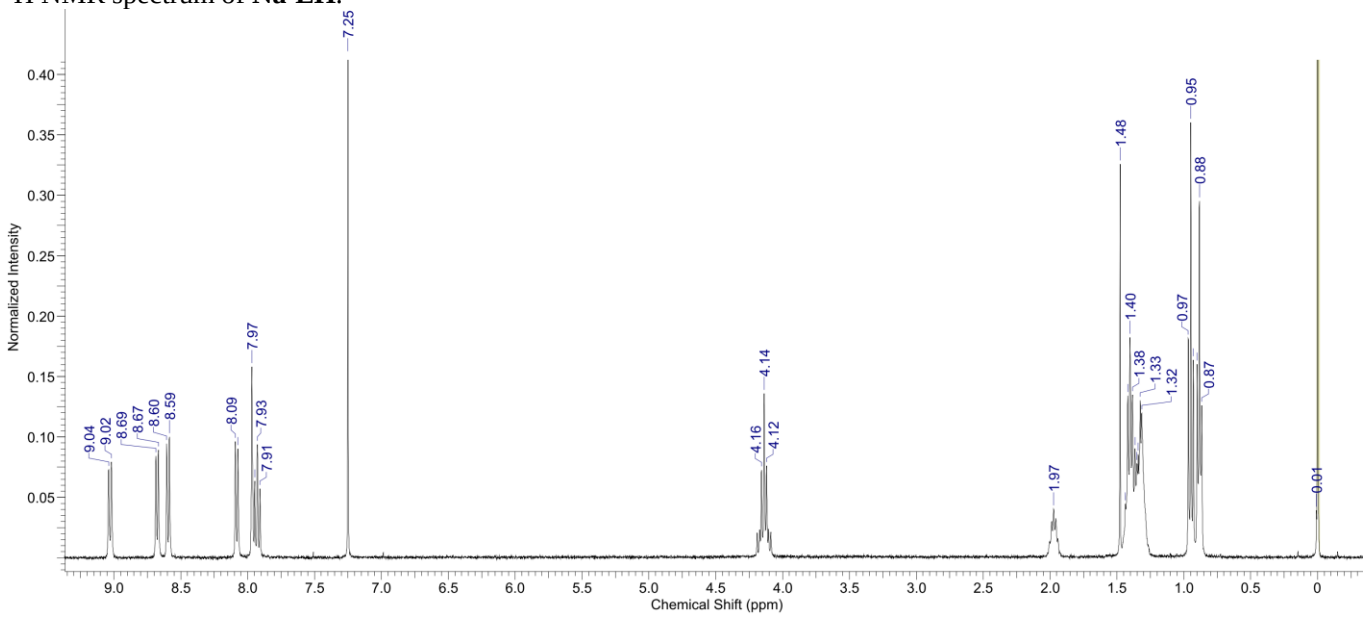

^{13}C NMR spectrum of **Na-EH**.

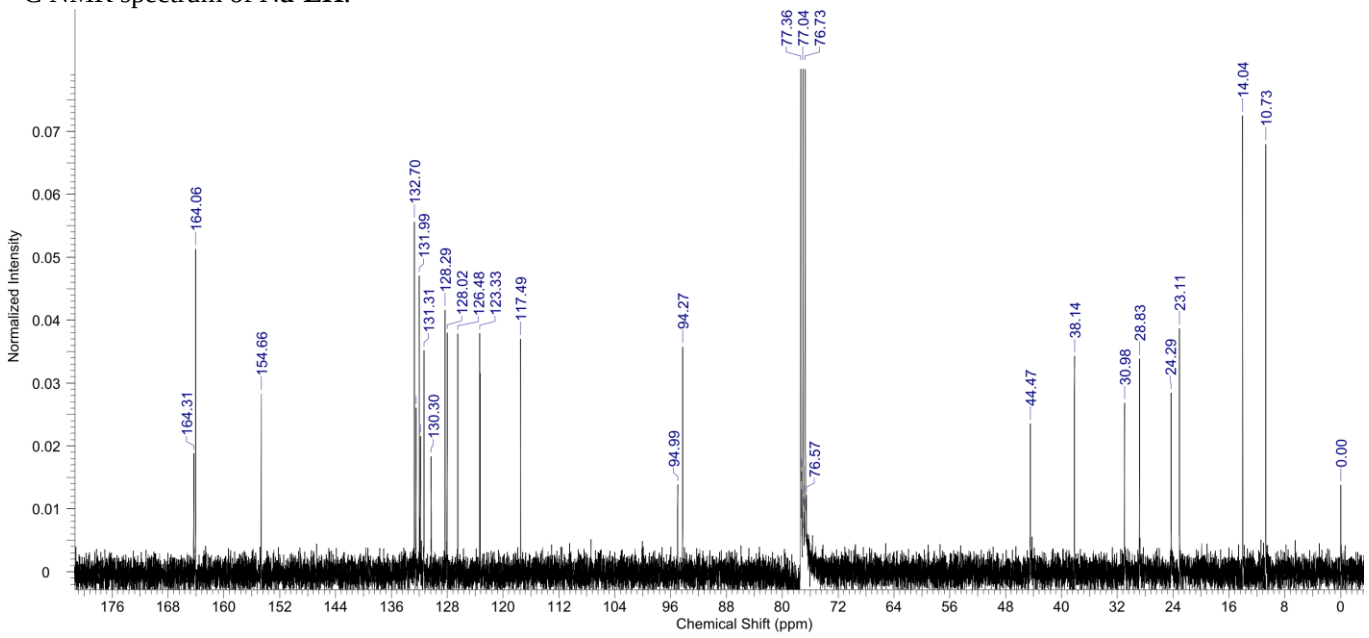

SCLC Measurements

Hole-only and electron-only devices were prepared with a structure of ITO/PEDOT:PSS/active layer/Au and ITO/TiO_x/active layer/Ca/Au, respectively. The active layers were prepared from 20 mg mL^{-1} solution of materials in $CHCl_3$. The carrier mobilities of these devices were calculated by the following equation:

$$J = \frac{9}{8}\varepsilon\varepsilon_0\mu\frac{V^2}{d^3}$$

where ε, ε_0, μ, and d are the dielectric constant of the active layer, the permittivity of free space, the carrier mobility, and the measured thickness of active layer, respectively. We used the values of $\varepsilon = 3$, $\varepsilon_0 = 8.8 \times 10^{-12}$.

SFE Estimation

The contact angles of film surface were measured by a NiCK LSE-ME1 using distilled water and glycerol. SFEs were estimated based on the theory established by Kaelble and Uy.[7]

PLQE Estimation

Blended films were prepared on the quartz substrate by spin-coating under identical condition of optimized active layers in OPVs. PLQE of blended films were calculated using following equation:

$$\mathrm{PLQE} = 1 - \frac{\phi_{p:n}}{\phi_p}$$

where Φ_p and $\Phi_{p:n}$ are the normalized photoluminescence intensities of reference and blended films at λ_{max}, respectively.

References

(1) Hadipour, A; Müller, R.; Heremans, P. *Org. Electron.* **2013**, *14*, 2379.

(2) Ie, Y,; Sato, C.; Nitani, M.; Tada, H.; Aso, Y. *Chem. Lett.* **2014**, *43*, 1640.

(3) Ie, Y.; Jinnai, S.; Nitani, M.; Aso, Y. *J. Mater. Chem. C* **2013**, *1*, 5373.

(4) Leu, W. C. W.; Fritz, A. E.; Digianantonio, K. M.; Scott Hartley, C. *J. Org. Chem.* **2012**, *77*, 2285.

(5) Gudeika, R; Lygaitis, R.; Mimaite, V.; Grazulevicius, J. V.; Jankauskas, V.; Lapkowski, M.; Data, P. *Dyes and Pigments* **2011**, *91*, 13.

(6) Jaeschke, G.; Jolidon, S.; Lindemann, L.; Ricci, A.; Rueher, D.; Stadler, H.; Vieira, E. *U.S.* **2012***/270852*.

(7) Kaelble, D. H.; Uy, K. C. *J. Adhesion* **1970**, *2*, 50.

Computational Details

All calculations were conducted using Gaussian 09 program. The geometry was optimized with the restricted Becke Hybrid (B3LYP) at 6-31 G(d, p) level.

Optimized structure of Ph-Me

Center Number	Atomic Number	Atomic Type	Coordinates (Angstroms) X	Y	Z
1	6	0	-0.724505	1.401759	0.012541
2	6	0	0.724645	1.401561	0.012484
3	6	0	1.458339	0.161631	0.015850
4	6	0	0.706853	-1.007391	0.019901
5	6	0	-0.707362	-1.007197	0.019917
6	6	0	-1.458534	0.162028	0.015897
7	7	0	-1.260589	2.624692	0.008986
8	16	0	0.000380	3.679781	0.005767
9	7	0	1.261061	2.624348	0.008886
10	6	0	2.871889	0.153411	0.013824
11	6	0	-2.872086	0.154187	0.013872
12	6	0	4.088877	0.152343	0.010658
13	6	0	-4.089073	0.153254	0.010707
14	6	0	5.509462	0.168553	0.005146
15	6	0	-5.509660	0.169189	0.005102
16	6	0	6.238546	-1.044752	0.007999
17	6	0	7.617741	-0.965980	0.002097
18	6	0	8.286971	0.260543	-0.007875
19	6	0	7.591518	1.461958	-0.011815
20	6	0	6.197085	1.405839	-0.004394
21	6	0	-6.197538	1.406330	-0.004867
22	6	0	-7.591981	1.462155	-0.012384
23	6	0	-8.287192	0.260600	-0.008098
24	6	0	-7.617707	-0.965780	0.002275
25	6	0	-6.238497	-1.044265	0.008292
26	6	0	8.640476	-2.057318	0.000973
27	7	0	9.882514	-1.406187	-0.010315
28	6	0	9.754855	-0.006959	-0.016465
29	6	0	-9.755021	-0.007221	-0.016692
30	7	0	-9.882386	-1.406466	-0.010123
31	6	0	-8.640206	-2.057337	0.001360
32	8	0	-8.474941	-3.260448	0.003521
33	8	0	-10.678932	0.781178	-0.032606
34	8	0	10.678582	0.781661	-0.032125
35	8	0	8.475492	-3.260467	0.002883
36	6	0	11.157978	-2.099384	-0.010563
37	6	0	-11.157710	-2.099923	-0.010370
38	1	0	1.227403	-1.958912	0.022606
39	1	0	-1.228170	-1.958578	0.022592
40	1	0	5.727572	-2.001048	0.014403
41	1	0	8.117909	2.410614	-0.020457
42	1	0	5.612980	2.319778	-0.006380
43	1	0	-5.613623	2.320389	-0.007157
44	1	0	-8.118564	2.410702	-0.021324
45	1	0	-5.727329	-2.000454	0.014946
46	1	0	11.032972	-3.057814	-0.516155
47	1	0	11.889180	-1.481790	-0.533777

48	1	0	11.510674	-2.279479	1.010058
49	1	0	-11.888532	-1.483717	-0.535758
50	1	0	-11.031765	-3.059388	-0.513751
51	1	0	-11.511554	-2.277906	1.010224

Optimized structure of Th-Me

Center Number	Atomic Number	Atomic Type	Coordinates (Angstroms) X	Y	Z
1	6	0	-0.724330	0.931722	0.000049
2	6	0	0.724346	0.931711	0.000062
3	6	0	1.457733	-0.308580	0.000063
4	6	0	0.706411	-1.479282	0.000057
5	6	0	-0.706435	-1.479270	0.000038
6	6	0	-1.457738	-0.308556	0.000037
7	7	0	-1.260329	2.154195	0.000049
8	16	0	0.000027	3.209779	0.000061
9	7	0	1.260364	2.154175	0.000072
10	6	0	2.868794	-0.315394	0.000068
11	6	0	-2.868800	-0.315346	0.000023
12	6	0	4.087759	-0.309915	0.000025
13	6	0	-4.087765	-0.309860	0.000041
14	6	0	5.488551	-0.303245	-0.000003
15	6	0	-5.488557	-0.303208	0.000035
16	6	0	6.338921	0.797807	-0.000151
17	6	0	7.687614	0.394573	-0.000193
18	6	0	7.870050	-0.966739	-0.000082
19	16	0	6.391776	-1.832282	0.000093
20	16	0	-6.391763	-1.832256	-0.000046
21	6	0	-7.870048	-0.966732	0.000089
22	6	0	-7.687628	0.394582	0.000170
23	6	0	-6.338941	0.797834	0.000142
24	6	0	-9.318931	-1.288799	-0.000123
25	7	0	-9.950819	-0.030306	-0.000093
26	6	0	-9.034941	1.039300	0.000085
27	6	0	9.034919	1.039307	-0.000209
28	7	0	9.950809	-0.030288	-0.000040
29	6	0	9.318937	-1.288789	0.000057
30	8	0	9.326282	2.216719	-0.000360
31	8	0	9.887769	-2.360133	0.000190
32	8	0	-9.326319	2.216709	0.000153
33	8	0	-9.887751	-2.360150	-0.000274
34	6	0	11.393230	0.136706	0.000078
35	6	0	-11.393242	0.136671	-0.000184
36	1	0	1.226593	-2.430978	0.000061
37	1	0	-1.226633	-2.430958	0.000027
38	1	0	5.980248	1.818758	-0.000227
39	1	0	-5.980280	1.818789	0.000200
40	1	0	11.596283	1.208004	-0.002625
41	1	0	11.833268	-0.321102	0.889913
42	1	0	11.833675	-0.325859	-0.887054
43	1	0	-11.596306	1.207970	-0.000089
44	1	0	-11.833413	-0.323422	-0.888756
45	1	0	-11.833543	-0.323623	0.888217

Optimized structure of Py-Me

Center Number	Atomic Number	Atomic Type	Coordinates (Angstroms) X	Y	Z
1	6	0	0.723996	1.246258	-0.000042
2	6	0	-0.724308	1.245905	-0.000438
3	6	0	-1.456871	0.005653	-0.000660
4	6	0	-0.706700	-1.164174	-0.000643
5	6	0	0.707548	-1.163829	-0.000483
6	6	0	1.457155	0.006360	-0.000103
7	7	0	1.259937	2.469185	0.000354
8	16	0	-0.000709	3.523860	-0.000300
9	7	0	-1.260842	2.468571	-0.000351
10	6	0	-2.870508	0.000205	-0.000933
11	6	0	2.870796	0.001606	0.000327
12	6	0	-4.087384	0.007460	-0.001228
13	6	0	4.087671	0.009088	0.000809
14	6	0	-5.504668	0.048833	-0.002116
15	6	0	5.504973	0.049939	0.001949
16	6	0	-6.282770	-1.129310	0.006491
17	6	0	-7.653733	-0.957792	0.005790
18	6	0	-8.198167	0.326702	-0.005158
19	7	0	-7.498836	1.457546	-0.014814
20	6	0	-6.171132	1.302782	-0.012323
21	6	0	6.171878	1.303647	0.012546
22	7	0	7.499637	1.457933	0.015340
23	6	0	8.198569	0.326841	0.005590
24	6	0	7.653679	-0.957456	-0.005743
25	6	0	6.282654	-1.128481	-0.006758
26	6	0	-8.772549	-1.947751	0.012032
27	7	0	-9.946025	-1.184211	0.004699
28	6	0	-9.698958	0.202422	-0.006612
29	6	0	9.699316	0.202025	0.007331
30	7	0	9.945890	-1.184695	-0.004217
31	6	0	8.772142	-1.947813	-0.011948
32	8	0	8.713411	-3.160651	-0.016917
33	8	0	10.550748	1.061774	0.021518
34	8	0	-10.550087	1.062477	-0.020443
35	8	0	-8.714251	-3.160611	0.016753
36	6	0	-11.281062	-1.757211	0.011883
37	6	0	11.280719	-1.758180	-0.011231
38	1	0	-1.227227	-2.115672	-0.000818
39	1	0	1.228536	-2.115076	-0.000518
40	1	0	-5.824221	-2.112145	0.013299
41	1	0	-5.574000	2.210819	-0.019055
42	1	0	5.575067	2.211895	0.019337
43	1	0	5.823756	-2.111150	-0.013881
44	1	0	-11.231980	-2.750592	-0.435129
45	1	0	-11.667472	-1.842453	1.032388
46	1	0	-11.943467	-1.108838	-0.563261
47	1	0	11.231235	-2.751542	0.435781
48	1	0	11.667227	-1.843567	-1.031687
49	1	0	11.943277	-1.110035	0.563994